



Shale barrier performance in petroleum systems: implications for CO₂ storage and nuclear waste disposal

Quentin Fisher^{1,2*}, Ieva Kaminskaite³ and Adriana del Pino Sanchez²

¹ School of Earth and Environment, University of Leeds, Leeds LS2 9JT, UK

² PetriVA Ltd., University of Leeds, Leeds LS2 9JT, UK

³ Institute of Petroleum Resources Exploration and Application, School of Earth Science, Northeast Petroleum University, China

QF, 0000-0002-2881-7018

* Correspondence: Q.J.Fisher@leeds.ac.uk

Abstract: Shale is often required to act as a natural barrier to fluid flow around nuclear waste repositories and above CO₂ storage sites. The small pore size of the shale matrix makes it an effective barrier to fluid flow. However, leakage could occur along faults or fractures. Experiments provide insight into fault/fracture-related leakage on short timescales (i.e. 1–10 years) compared to that needed for safe disposal (up to 1 Ma). Data collected by the petroleum industry provides strong evidence on how faults and fractures in shale impact fluid flow on such timescales. Faulted shales act as seals to petroleum reservoirs and abnormal pressures on geological timescales (>10 Ma). This observation suggests that faults in shale can either form without acting as flow conduits or act as temporary conduits but then reseal. Index properties such as clay content and elastic moduli are useful for identifying shales in which faults/fractures are likely to self-seal. However, fault and fracture-related fluid flow can occur through weak shales if high overpressures are maintained. Nuclear waste repositories can be sited away from where overpressures could develop. Leakage from CO₂ storage sites is more risky because the CO₂ provides drive to maintain high pressures, which could suppress self-sealing.

Thematic collection: This article is part of the Fault and top seals 2022 collection available at: <https://www.lyellcollection.org/topic/collections/fault-and-top-seals-2022>

Received 13 February 2023; **revised** 1 November 2023; **accepted** 3 November 2023

The need to reduce greenhouse gas emissions has increased the urgency to use the subsurface for the safe disposal of waste products (e.g. nuclear materials, CO₂) and the storage of fuel (e.g. hydrogen) and energy (e.g. compressed air, geothermal). To gain a social licence for subsurface disposal or storage, it is mandatory to build a safety case consisting of a set of arguments supported by critically-appraised evidence that conclusively demonstrates significant leakage is unlikely over the timescale of interest. The time-scale over which leakage risk needs to be assessed ranges from days in the case of gases that can cause combustion (e.g. hydrogen, methane) or asphyxiation (e.g. CO₂) and up to 1 Ma for nuclear waste. In most cases, natural barriers such as shales are required to prevent leakage from disposal and storage sites (hereinafter referred to as disposal sites). Shale is one of the most important barriers to fluid flow in the subsurface; it generally accounts for over 50% of the rocks within sedimentary basins (e.g. Ronov 1983) and is known to have extremely low permeability (e.g. Neuzil 1994, 2019). Indeed, shale is the primary seal to several current experimental/operational (e.g. Sleipner – Furre *et al.* 2017; In Salah – Ringrose *et al.* 2013) and future CO₂ (e.g. Northern Lights project – Jackson *et al.* 2022) storage sites. It is also considered by several countries (e.g. Belgium, France, Switzerland) as the preferred host lithology for deep geological repositories for nuclear waste.

A key issue when assessing the ability of a shale for a storage site to act as a robust seal is that its behaviour needs to be predicted on timescales that are far longer than can be observed directly in laboratory experiments or within subsurface test sites. For example, it is only practical to run experiments for a small number of years whereas barriers to nuclear waste disposal need to prevent significant leakage for up to 1 Ma. As an example of ‘significant’ leakage, current regulation in Switzerland stipulates that humans

should not receive a dose of >0.1 mSv per year (Brennwald and Van Dorp 2009), which is around 1/25th of current background levels. It is possible to extrapolate experiments to longer timescales but this inevitably adds uncertainty to the estimates of long-term shale barrier performance. A complementary route to understand the long-term behaviour of shale is by observing how it has impacted fluid flow over geological timescales. Fortunately, the petroleum industry has gathered extensive data, which provide evidence for how shales have impacted fluid flow over a wide range of timescales (days to >100 Ma). For example, the petroleum industry has extensive evidence regarding the ability of shale to act as a long-term seal to petroleum reservoirs and abnormally pressured compartments. The aim of this paper is to review these data and assess implications for predicting the ability of shale to act as a safe natural barrier that prevents leakage from subsurface disposal sites. A particular emphasis is placed on nuclear waste disposal and CO₂ storage but the same arguments are relevant for risking hydrogen and pumped air storage.

Much of the paper is dedicated to highlighting evidence of shale barrier performance obtained from conventional petroleum reservoirs and abnormally pressured compartments. We have also included a discussion of shale resource plays because they provide evidence of how very strong fine-grained rocks that deform in a brittle manner impact fluid flow. The examples from the petroleum industry cover a wide range of burial depths (250 to 6000 m), which means that they are good analogues for CO₂ storage sites, which generally need to be more than 500 m below the seabed to achieve the pressure and temperature conditions for CO₂ to act as a dense phase (e.g. Lindeberg *et al.* 2009). Disposal sites for CO₂ can, however, be considerably deeper. For example, the Northern Lights project is currently assessing storage sites at a depth of 2000–

3000 m, offshore Norway. On the other hand, shale-hosted repositories for nuclear waste are likely to be confined to a more restricted depth range that is sufficient to ensure waste materials do not reach the biosphere but also sufficiently shallow to allow tunnelling to occur (Horseman 1994; Sellin and Leupin 2014). For example, in 2022 the National Cooperation for the Disposal of Radioactive Waste (NAGRA) in Switzerland announced that their preferred site for a nuclear waste repository was in the Opalinus Clay at a depth of ~800 m in the Nördlich Lägern area.

The review begins by defining what is meant by shale in the context of the current paper. The paper then describes evidence on how shales impact fluid flow in the subsurface that has been gathered during the exploration, appraisal and production of petroleum reservoirs. Key evidence discussed includes the ability of shale to act as seals to conventional petroleum reservoirs and abnormally pressured compartments. The paper also reviews data gathered from shale resource plays and assesses its implications for shale barrier performance. The methods that are used by the petroleum industry to predict subsurface flow through shale are then described. Finally, implications of the evidence presented for the ability of shale to act as a safe, long-term, natural barrier that prevents leakage from subsurface disposal sites is discussed. Strong arguments can be made that the matrix properties of shale prevent significant focused fluid flow on the time scales of interest to subsurface waste disposal. Much of the review therefore focuses on the controls on leakage through shale via natural faults and fractures.

What is a shale?

Fine-grained sedimentary rocks are generally defined as being dominated by grains with a size <62.5 μm (Blatt 1982; Lazar *et al.* 2015; Ilgen *et al.* 2017). There is still considerable debate regarding both the classification and terminology associated with these rocks (e.g. Milliken 2014; Lazar *et al.* 2015; Camp *et al.* 2016). For example, shale has often been used to refer to indurated, laminated and fissile, fine-grained, sedimentary rock containing a high proportion of clay (e.g. Ilgen *et al.* 2017). The term ‘clay’ in itself has been used to describe a particular grain-size or mineralogy. Most geologists use the term clay to describe particles of <2 μm whereas sedimentologists use clay for grains with a size of <4 μm (Guggenheim and Martin 1995). Clay minerals are defined by most geologists as phyllosilicates with a grain-size of <2 μm (Moore and Reynolds 1997; Huggett 2005). Although Guggenheim and Martin (1995) argued that clay mineral should refer to any mineral that that imparts plasticity on a material with a high water content. Prior to the rapid expansion of the shale gas industry in the early 2000’s, most geoscientists thought of shale as containing a large proportion of clay minerals (i.e. >60%). However, in the context of unconventional petroleum production, the term shale is commonly used to describe a range of lithologies including fine-grained marls and quartz-rich siltstones. The term shale is used in this paper to cover the full range of fine-grained, clay-bearing lithologies, which act as caprocks to petroleum reservoirs, seals to overpressured compartments and reservoirs for petroleum in shale resource plays (i.e. gas and oil shales).

Controls on fluid flow through shale matrix

The non-turbulent flow of a single-phase fluid in a porous media is generally calculated using Darcy’s Law:

$$Q = \frac{kA}{\mu} \frac{dP}{dL} \quad (1)$$

where: Q is the volumetric flow rate ($\text{cm}^3 \text{s}^{-1}$), A is the flow area perpendicular to flow (cm^2), k is the permeability (Darcy), μ is the fluid viscosity (Pa.s), dL is the flow path length (cm) and dP is the

fluid potential across rock sample (atm.). In rocks with very small pore throat-sizes (i.e. less than 1 μm), gas transport can be dominated by other flow mechanisms such as slippage, transitional flow and Knudsen diffusion particularly when gas pressures are low (Freeman *et al.* 2011). It has also been suggested that departures from Darcy’s law can occur at very low flow rates, a process known as pre-Darcy flow (e.g. Longmuir 2004). A consequence of pre-Darcy flow is that a threshold pressure gradient is required to initiate single-phase flow (Prada and Civan 1999). The threshold pressure gradient increases as permeability decreases and therefore is likely to be particularly important for fluid flow in shale (Yang *et al.* 2022). A key issue related to published shale permeability values is that it is likely that most samples have not been preserved or handled properly prior to testing. For example, Ewy (2015) argued that exposing shales to water when not stressed will damage their microstructure and therefore invalidate later laboratory testing. It is also the case that drying samples results in significant capillary suction, which can reduce permeability and the stress dependence of permeability.

Capillary pressure also impacts fluid flow when two or more immiscible fluids are present. In particular, for a non-wetting phase to pass through a pore throat its phase pressure needs to be higher than that of the wetting fluid by an amount known as the capillary entry pressure, P_c . Capillary entry pressure can be estimated from the pore throat size of the rock and the interfacial tension of the brine-petroleum system using the Young-Laplace equation:

$$P_c = \frac{2\gamma \cos \theta}{r} \quad (2)$$

where: γ is the interfacial tension between petroleum and water; θ is the contact angle between the fluids and rock surface, and r is pore throat radius. A rock usually consists of a range of pore throat sizes and the minimum pressure that is necessary for a non-wetting fluid to completely pass through its pore system is controlled by the minimum pore throat radius along the path joining the largest connected pore throats; this is often referred to as the threshold pressure, P_{th} (Katz and Thompson 1986, 1987).

Shale is a particularly effective barrier to fluid flow because it has small pores, leading to very low permeability and high threshold pressure. Measuring shale permeability is difficult for several reasons (e.g. Passey *et al.* 2010; Boulin *et al.* 2012; Fisher *et al.* 2017; Neuzil 2019) such as: (i) the lengthy times required for pressure equilibrium to occur; (ii) the difficulty in measuring low flow rates in steady-state experiments; (iii) the sensitivity to small leaks during transient flow experiments; (iv) the difficulty in obtaining undamaged, preserved, samples; (v) the sensitivity of measurements to saturation and brine composition; etc. Caution should therefore be taken when using shale permeability data. However, a compilation of several major sources of shale porosity and permeability data seem to indicate that shales similar to those discussed in this review have permeabilities of 100 to <0.1 nD (Fig. 1). Neuzil (2019) showed that the permeability of homogenous clay-rich shales measured in laboratory tests was consistent with values measured from packer tests in boreholes. However, packer tests conducted in more heterogeneous sequences gave permeabilities that are often many orders of magnitude higher than those measured in the laboratory.

Capillary pressure tests on shale using the gas-brine or oil-brine systems are generally slow so there are only a limited amount of experimental data available. There are some notable exceptions. For example, Ito *et al.* (2011) measured N_2 -air threshold pressures of between 123 and 508 psi. Andra (2009) measured gas breakthrough pressures of 580 to 725 psi. Amann-Hildenbrand *et al.* (2013) measured CO_2 -brine and He-brine capillary pressures of 725 to 1900 psi. It is far more common to estimate threshold pressures of shale using mercury injection porosimetry (MIP)

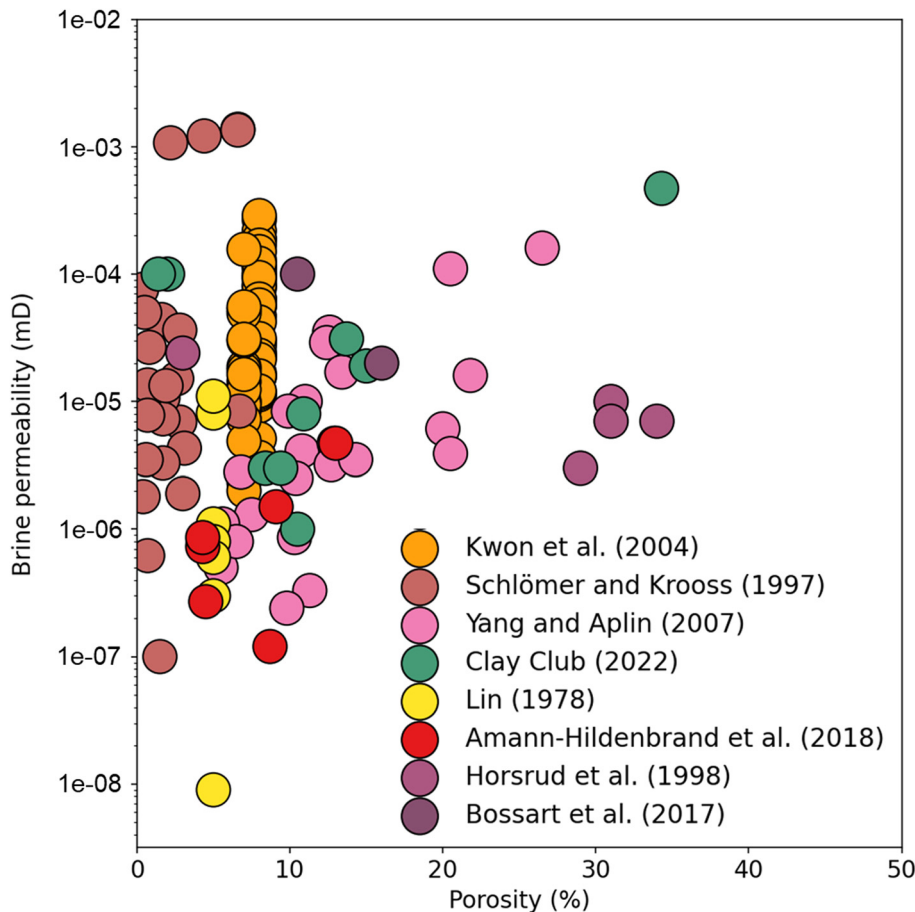


Fig. 1. Plot of porosity v. permeability for a range of shale samples. All measurements are approximately *in situ* stress using brine permeametry (steady-state or transient methods). Many of the samples have not been preserved adequately so the data need treating with some caution.

because the incompressible nature of the mercury allows measurements to be conducted rapidly (<1 day). MIP analysis indicates that shales generally have Hg-threshold pressures of 100 to 2100 psi 0.69 to 14.5 MPa when converted to the air-brine system (Almon *et al.* 2005). It should, however, be noted that the use of MIP data to determine threshold pressures of shale samples is controversial for a number of reasons. Firstly, it is possible that the mercury will damage delicate clay structures present in shale (Horseman *et al.* 1996). Secondly, MIP analysis is conducted on samples that have generally been dried to 105°C, which will also damage the clay matrix (Delage and Lefebvre (1984). Thirdly, experiments, such as those that have attempted to inject Wood's metal into shale have been interpreted to suggest that mercury may not actually enter the pore space of shale (Hildenbrand and Urai 2003). Finally, the industry-standard method for MIP does not measure mercury breakthrough and instead the threshold pressure is estimated from the shape of the injection pressure v. mercury saturation curve, which is often quite arbitrary (Schlömer and Krooss 1997). Indeed, although good correlations between gas-brine breakthrough tests and MIP results have been noted for porous sandstones and carbonates (e.g. Thomas *et al.* 1968) these measurements have been shown to be uncorrelated when performed on shale (Hildenbrand and Urai 2003).

The density contrast between petroleum and water has a large influence on the buoyancy force within the petroleum column and hence the pressure differential (capillary pressure) between the petroleum and water at the interface of the reservoir and seal. The density of brine varies between around 1000 and 1200 kg m⁻³. The density of petroleum shows far larger variations, from <200 kg m⁻³ for a dry gas to >900 kg m⁻³ for a very heavy oil. Dense phase CO₂ is likely to have a density of ~700 kg m⁻³. To place these figures in context, typical shales could seal a dense phase CO₂ column of 250 to 6500 m assuming CO₂ and brine densities of 700 and

1050 kg m⁻³ respectively and using a CO₂-brine interfacial tension value of 0.030 N m⁻¹. It should be noted that, to the authors' knowledge, there do not exist good datasets to demonstrate that capillary pressure measurements have successfully predicted the column heights that have been sealed in the subsurface.

Evidence of shale barrier performance from petroleum systems

Shale caprocks to petroleum reservoirs

Over 50% of the world's largest oil and gas fields are capped by shale (Grunau 1987). In general, shale caprocks to petroleum reservoirs are clay-rich. For example, bulk mineralogical data derived from X-ray diffraction analysis (XRD) shows that shale caprocks to petroleum reservoirs on the Norwegian and UK continental shelf (Fig. 2) mainly contain >40% clay although they do contain some horizons with lower clay contents possibly due to the presence of siltstone layers.

Shale caprocks to petroleum reservoirs frequently contain faults on a range of scales, some of which are seismic-scale. Indeed, three-way dip closures, in which the petroleum is trapped due to across-fault juxtaposition of the reservoir against shale, are one of the most common types of conventional petroleum trap. For example, Spencer and Larsen (1990) estimated that 70% of the petroleum discoveries in the northern North Sea, where shale is the most common caprock, were within fault-bounded blocks. The observation that extensively faulted shale sequences can seal petroleum over geological timescales of >10 Ma (e.g. Karlsen and Skeie 2006; Bourdet *et al.* 2020) and sometimes in excess of 100 Ma (e.g. Miller 1992; MacGregor 1996; Zhu *et al.* 2013) provides strong evidence that faults in shale can either: (i) develop without acting as significant conduits to fluid flow, or (ii) act as temporary conduits to

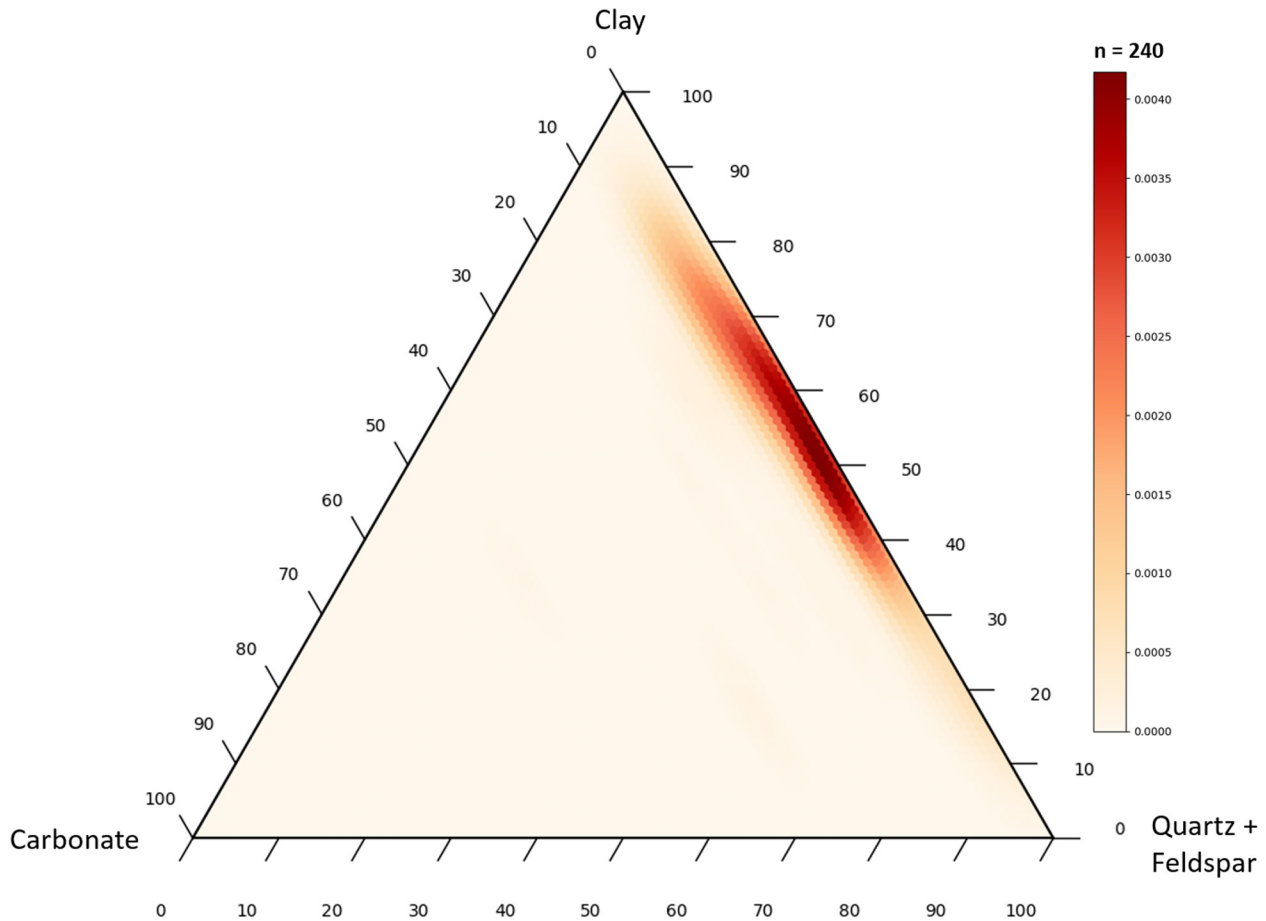


Fig. 2. Mineralogical composition of shale caprocks from the UK and Norwegian continental shelves. Data includes proprietary data collected by the University of Leeds as well as values published in Lu (2008), Fishman *et al.* (2012), Kalani *et al.* (2015). The scale is the probability density function (see Scott 1992). It is a measure of the density of data within a given area of the ternary plot.

fluid flow but can then reseal sufficiently that they are able to support very significant petroleum columns.

The petroleum industry does, however, frequently drill traps beneath shale caprocks, which prove to be underfilled or dry due to leakage of the petroleum (e.g. Gaarenstroom *et al.* 1993; Nordgård Bolås and Hermanrud 2003). Threshold pressure measurements described above suggest that shale caprocks can seal very large petroleum columns indicating that capillary flow through the shale matrix is not always responsible for leakage (e.g. Schofield 2016). Instead, it can be argued that leakage from petroleum reservoirs, which are capped by shales, has occurred along fractures (e.g. Gaarenstroom *et al.* 1993) or faults (e.g. Losh 1998; Castillo *et al.* 2000; Losh *et al.* 2002). Compelling evidence to indicate that faults have acted as conduits to petroleum includes the presence of gas clouds (Cartwright *et al.* 2007), diagenetic-related zones (O'Brien and Woods 1995; O'Brien *et al.* 1998), as well as mapped lineaments of petroleum seeps and pockmarks (Løseth *et al.* 2009) positioned directly above faults within the shale caprock. It should be noted that despite having leaked hydrocarbons, dry structures are frequently highly overpressured (Gaarenstroom *et al.* 1993). In cases where leakage occurred along faults and/or fractures, the retention of high overpressures provides strong evidence of their ability to self-seal (Engelder and Leftwich 1997).

It is frequently observed that the maximum pore pressure measured in the subsurface approximately coincides with the minimum horizontal stress, S_{hmin} , (e.g. Gaarenstroom *et al.* 1993; Engelder and Fischer 1994; Hillis 2001; Tingay *et al.* 2009; Swarbrick *et al.* 2010). This has been interpreted as evidence that natural vertically oriented hydraulic fractures are formed when the

pore pressure exceeds S_{hmin} allowing leakage to occur. Uncertainties such as the extent of coupling between horizontal stress and pore pressure (e.g. Hillis 2001; Swarbrick and Lahann 2016) and whether or not the tensile strength or other fracture initiation criteria need to be exceeded for natural vertically oriented hydraulic fractures to form means that it is not always certain whether leakage occurred along faults or fractures (Engelder and Leftwich 1997). The key point relevant to the current review is that high pore pressures can result in the formation of dilatant pathways for fluid flow through shale, which self-seal as pore-pressures decrease.

Key concepts related to top seal leakage include lateral pressure transfer (e.g. Yardley and Swarbrick 2000), protected traps and leakage through the shallower structures within a pressure cell (e.g. Winefield *et al.* 2005). Here brine from compacting shales is expelled into higher permeability carrier beds where it flows up-dip. The transfer of pressure leads to the fracture pressure being reached in the shallowest structures within the pressure cell whereas the deeper structures do not reach fracture pressure and are therefore protected from leakage (e.g. Fig. 3).

Seal integrity during uplift

Considering the timescales over which disposal sites need to remain undisturbed it is necessary to assess whether their integrity could be impacted by long-term processes such as glaciation, uplift and erosion. Fortunately, there is a significant amount of information on how glaciation impacts the integrity of caprocks to petroleum reservoirs. The Barents Sea on the Norwegian continental

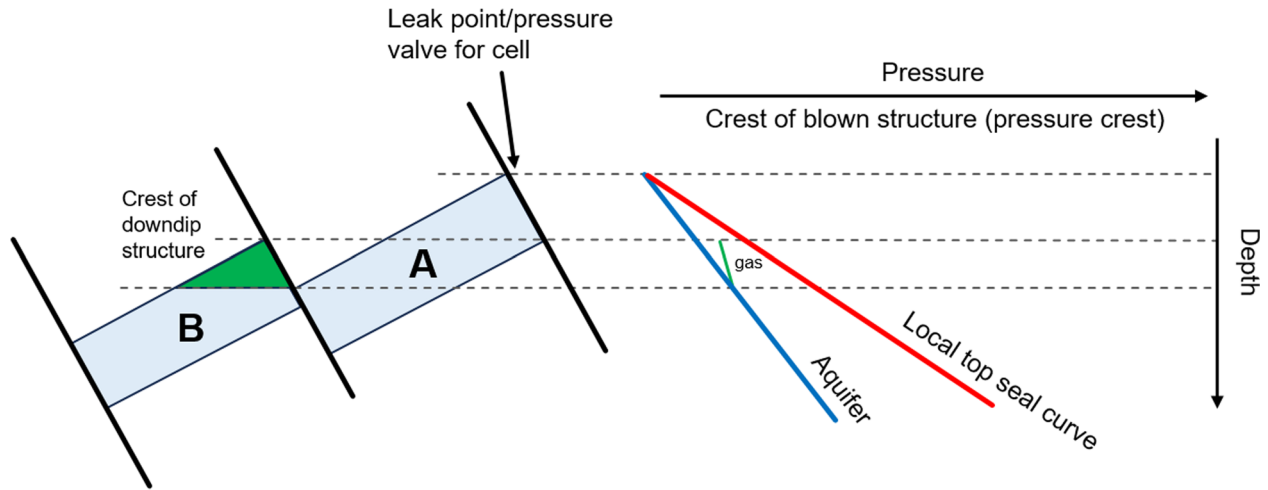


Fig. 3. Diagram highlighting the concept of regional leak points and protected traps (adapted from Winefield *et al.* 2005). The aquifer pressure within the shallowest structure reaches the fracture pressure allowing leakage. The aquifer pressure in the deeper compartment does not reach fracture pressure and therefore leakage does not occur.

shelf is a particularly good area to assess the role of glaciation, uplift and erosion on caprock leakage. Here the reservoirs have had up to 3 km of overburden removed due to uplift and erosion after charging with petroleum (Doré *et al.* 2000; Ohm *et al.* 2008; Henriksen *et al.* 2011). The region has also experienced over 40 glacial cycles each likely to have produced rapid changes in pore pressures, temperature and stress (e.g. Nøttvedt *et al.* 1988; Ostanin *et al.* 2017). Kishankov *et al.* (2022) argue that up to 20% of the oil and gas in the northern Barents Sea was lost during the first episode of deglaciation due to loss of mechanical seal integrity via fracturing or fault reactivation. Ohm *et al.* (2008) also argue that gas has preferentially leaked from structures such as Goliat. Tasianan *et al.* (2016) used seismic anomalies as evidence that leakage has mainly occurred along large-scale faults reactivated possibly as a result of glacial loading and unloading. Ostanin *et al.* (2017) argue that faults leaked during ice retreat but self-sealed during glaciations and interglacial periods. Paulsen *et al.* (2022) suggested gas had preferentially escaped from the Wisting field, which now only contains oil. The leakage mechanism is not yet totally understood but the presence of amplitude anomalies above faults within the area is consistent with fault-related leakage. Overall, there still exists considerable debate regarding leakage mechanisms and the amount of leakage that has occurred in the Barents Sea. However, it seems likely that fault reactivation, possibly as a result of glacial cycles, has caused

periodic episodes of petroleum leakage and self-sealing in the Wisting field.

Shales as seals to abnormal pressure

Abnormal pressure has been defined as any pressure higher than that generated by a hydrostatic water column (Dickinson 1953). However, it is now widely recognized that subsurface pressures can be both higher (e.g. Osborne and Swarbrick 1997) and lower than the hydrostatic pressure (e.g. Birchall *et al.* 2022); these are referred to as overpressured and underpressured respectively. Standard pressure plots used in the petroleum industry (Fig. 4) display measured pore pressures as a function of depth. These often display hydrostatic (usually referred to as normal pressure) and lithostatic pressure gradients. The hydrostatic pressure gradient is a reference for overpressure (zero when pore fluids are actually normally pressured). The hydrostatic pressure gradient is typically around 0.45 psi ft^{-1} or 10 MPa km^{-1} when the pore fluid chemistry is similar to seawater. High salinities, associated with salt/evaporites in the stratigraphic sequence, may lead to hydrostatic gradients as high as 0.52 psi ft^{-1} or 12.0 MPa km^{-1} . The lithostatic pressure gradient, which commences at the rock surface onshore, or sea-bed offshore, typically has a value which increases downwards related to compaction. Typical values range from 0.8 psi ft^{-1} or 18.0 MPa km^{-1}

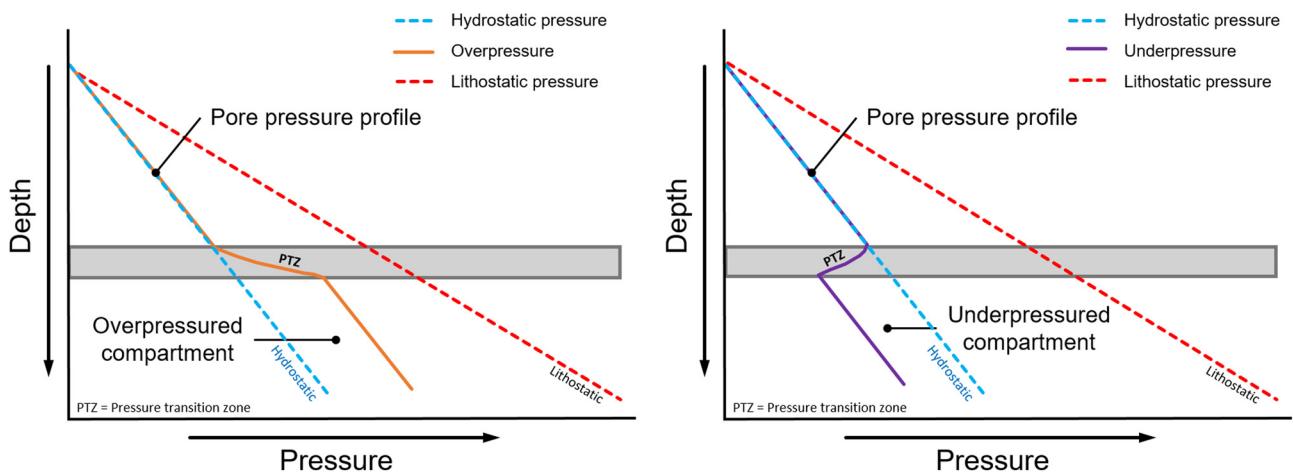


Fig. 4. Plots showing hydrostatic pressure, and lithostatic pressure gradients compared to pressure profiles for left) an overpressured compartment, and right) an underpressured compartment.

km^{-1} in shallow, uncompacted clay-rich sediment increasing to 1.0 psi ft^{-1} or 23 MPa km^{-1} or higher at depth. The shallow subsurface (i.e. $<1\text{--}2 \text{ km}$) is generally normally pressured but can be underpressured; overpressures are often observed at greater depths. The pressure to depth ratios of overpressured fluids range from just above hydrostatic to just below the lithostatic pressure gradient. Underpressures range from just below hydrostatic to as low as 1% of the hydrostatic pressure (Birchall *et al.* 2020).

It is difficult to obtain direct measurements of pore pressure in shale due to their low permeability. Instead, pore pressure measurements are often made in higher permeability lithologies such as sandstone that are present within the shale sequences and these are assumed to be representative of the enclosing shale. Pressure can be estimated indirectly using wireline log and/or seismic data assuming a relationship exists between velocities and compaction state. It is commonly observed that shale is present at the transition from normally pressured sediments in the shallow subsurface to overpressured sediments at depth (e.g. Dickinson 1953; Teige *et al.* 1999). It is often argued that the overpressure is either generated within the shale due to processes such as disequilibrium compaction, organic matter transformation, and mineral reactions (such as chemical compaction) or that the shales are providing the barrier that retards the dissipation of overpressure in reservoirs, which are generated by processes at greater depth such as the chemical compaction of sandstones (Osborne and Swarbrick 1997; Goult *et al.* 2016). Irrespective of the mechanism for overpressure generation, shale is acting as an effective barrier to fluid flow.

Underpressured sediments are found in many sedimentary basins throughout the world particularly those that have experienced uplift (Birchall *et al.* 2022). A range of processes may be responsible for the development of underpressure (Swarbrick and Osborne 1998) but thermal cooling (Birchall *et al.* 2020) and decompaction (e.g. Neuzil and Pollock 1983) are commonly cited causes. Underpressure is also reported from both within (e.g. Vinard *et al.* 2001) and beneath (e.g. Braathen *et al.* 2012) faulted shales.

Overall, abnormal pressures within and below heavily faulted shales indicates that even if the faults or fractures once provided conduits for fluid flow they have since self-sealed and barrier performance has not been totally compromised.

Evidence of sealing from shale resource play data

In the 10 years between 2005 and 2015, $>100\,000$ wells were drilled and hydraulically fractured in shale resource plays in North America to produce both gas and liquid hydrocarbons. The economically successful shale plays have a wide range of mineralogical compositions (Fig. 5). All contain significant ($>10 \text{ m}$) sections with a low clay content ($<40\%$ clay) with the remainder of the mineralogy being dominated by quartz-feldspar and/or carbonates. Static and dynamic data obtained during exploration, appraisal and production provide useful information from shales that can be viewed as the opposite end-member (i.e. clay-poor, strong and brittle) compared to the clay-rich shales that provide caprocks to petroleum reservoirs and barriers to overpressured compartments. A

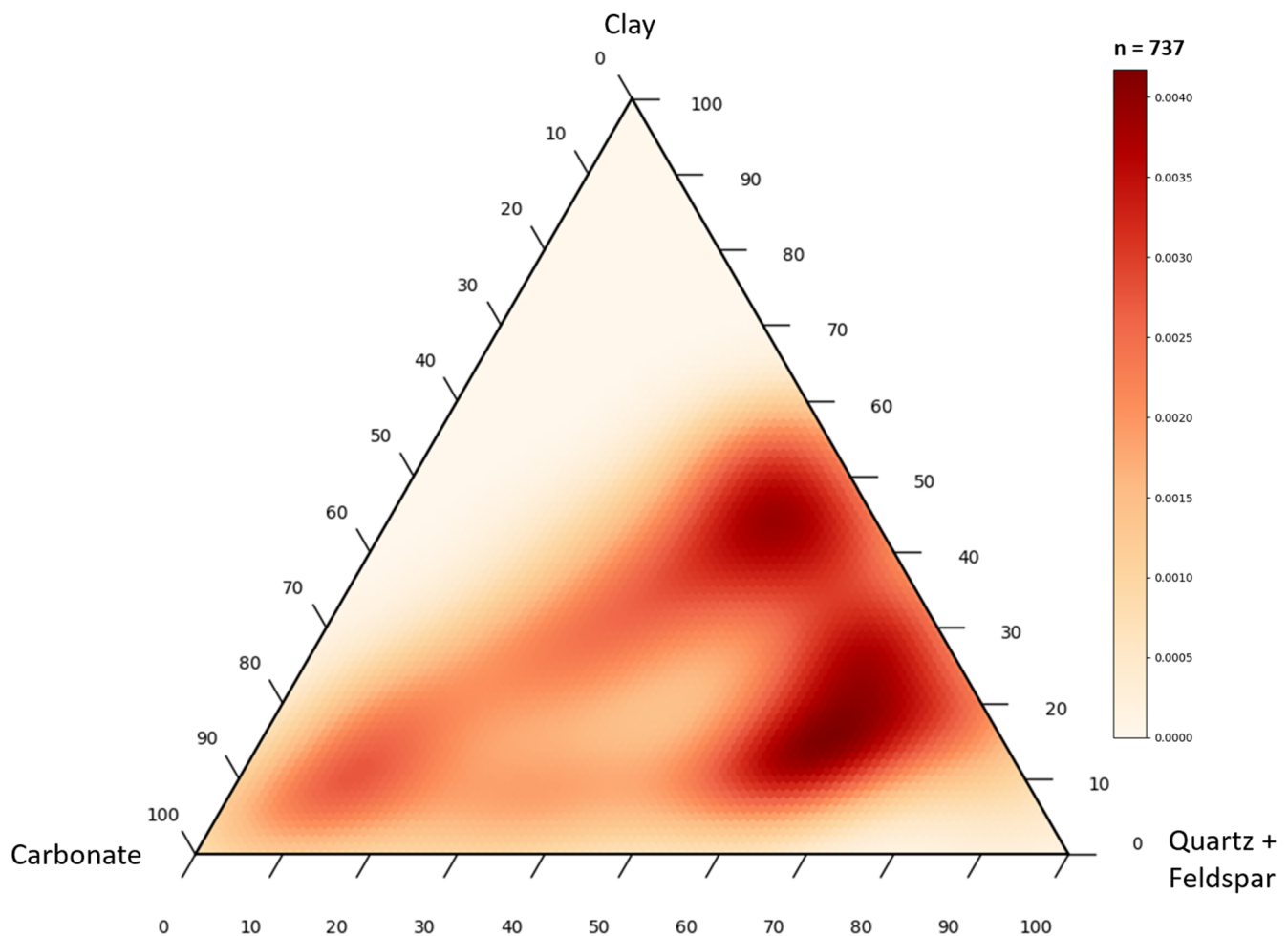


Fig. 5. Mineralogy of typical shale resource plays in North America (Mnich 2009; Chalmers and Bustin 2012; Egbobawaye 2016a, b; Prasad *et al.* 2016; Hupp and Donovan 2018; Smye *et al.* 2019; Unpublished proprietary data from Petrivu Ltd.). Shale plays represented include Barnett, Bakken, Eagleford, Fayetteville, Haynesville, Horn River, Marcellus, Montney and the Woodford. The scale is the probability density function (see Scott (1992)). It is a measure of the density of data within a given area of the ternary plot.

Table 1. Depth-pressure ratios (range and average), present-day burial depths and the amount of uplift experienced for shales plays within North America

Shale play	Pressure-depth ratio (psi/ft) (range and average)	Current burial depth (m)	Uplift (m)	Reference
Antrim	0.2–0.38 (0.30)	150–600	1200	Apotria <i>et al.</i> (1994)
Bakken	0.5–0.82 (0.66)	2900–3200	300	Webster (1984)
Barnett	0.53	1900–2600	1500	Bowker (2007); Montgomery <i>et al.</i> (2005)
Eagle Ford	0.4–0.8 (0.60)	2010–3700	1200	Pathak <i>et al.</i> (2015)
Fayetteville	0.44	300–2150	2000	Lamb (2014)
Haynesville	0.75–0.94 (0.85)	3200–4200	0	Nunn (2012)
Horn River	0.44–0.80	1800–3000	1000	Wilson and Bustin (2017)
Mancos	0.45–0.9 (0.68)	1520–2400	1800	Quick and Ressetar (2012)
Marcellus	0.4–0.8 (0.60)	1200–2600	3000	Evans (1995)
New Albany	0.43	150–1380	800	Strapoć <i>et al.</i> (2010)
Niobrara	0.41–0.67 (0.53)	1600–2600	1100	Crysdale and Barker (1990)
Utica	0.56–0.8 (0.68)	1200–4300	1800	Milici and Swezey (2014)
Wolfcamp	0.46–0.70 (0.6)	1650–3350	800	Friedrich and Monson (2013); Heij (2018)
Woodford	0.6–0.65 (0.63)	1800–4800	800	Pawlewicz (1989)

key reason for including shale plays in this review is that despite them being extremely stiff with less clay content than caprocks to petroleum reservoirs there is considerable evidence that they retain gas even when fractured and hydraulic fractures used to extract gas rarely extend a significant distance into the overburden.

Static data

Natural faults and fractures have been identified in most producing shale resource plays (Gale *et al.* 2014) yet by definition these rocks have been able to retain petroleum over geological timescales. The gas and oil within shale plays is generally self-sourced so the timing of petroleum generation can be estimated from their burial history. Some plays, such as the Haynesville, are currently at around their maximum burial depth and it seems likely that petroleum is still being generated (Nunn 2012) whereas gas in some shales (e.g. the Barnett shale) may have been generated >200 Ma ago (Montgomery *et al.* 2005).

Shale plays have a wide range of pressure to depth ratios ranging from 0.2 to 0.94 psi ft⁻¹ or 4.5 to 21.3 MPa km⁻¹ (Table 1). These cannot be directly translated to the extent of abnormal pressure

because the measurements are not aquifer pressures instead they represent the petroleum pressure. The shale plays with very high pressure to depth ratios would require unrealistically high gas columns for the reservoir to be classified as normally pressured. For example, even the Barnett shale with a pressure to depth ratio of 0.56 psi ft⁻¹ would require an unrealistically large gas column of nearly 700 m for brine to be normally pressured. We therefore refer to the shale plays with pressure to depth ratios of <0.45 psi ft⁻¹ as being underpressured whereas those with higher pressures to be high-pressured plays. The underpressured plays (e.g. Antrim and Ohio shale plays) are all shallowly buried and have experienced significant uplift whereas those with the highest pressure to depth ratio, for example, the Haynesville shale, is deeply buried and has experienced little uplift (Fig. 6). Uncertainties remain regarding the origin of high pressures within shale resource plays. However, in the context of the current article, high pressures within many of the shale resource plays, provides strong evidence that seal integrity has been maintained despite the fact that some of the shale plays reached maximum burial depth over 300 million years ago and have since experienced significant uplift.

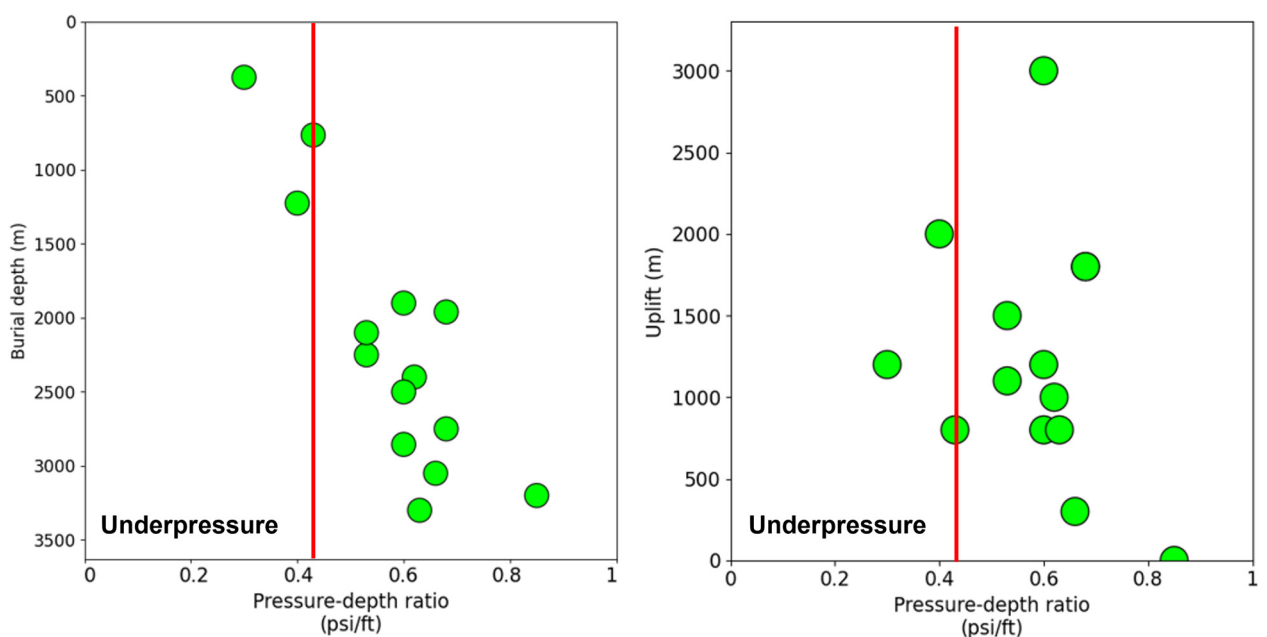


Fig. 6. Plots of left) burial depth, and right) uplift against pressure-depth ratio for major shale plays from North America. Data sources are provided in Table 1. The red-lines denote a normal pressure gradient.

The observation that overpressures exist within shale resource plays is not, however, evidence that leakage of petroleum has not occurred. Indeed, it is widely believed that petroleum in younger strata was sourced from the shale resource plays. For example, [Jarvie *et al.* \(2007\)](#) identified 13 petroleum accumulations containing oil that are believed to have been sourced from the Barnett shale. Also, geochemical analysis indicates that significant amounts of petroleum has been expelled from the shale gas resource plays (e.g. [Wood and Sanei 2016](#)).

The distribution of pressures may also provide evidence of leakage. Theoretically, it would be expected that uplift of gas-bearing shales would increase its pressure to depth ratio ([Bowers 1995](#); [Katahara and Corrigan 2004](#)). The reason for the increase in pressure to depth ratio is that uplift results in a small increase in porosity, which results in only a small decrease in gas pressure due to its high compressibility. The data provided in [Table 1](#) and [Figure 6](#) suggest that the opposite occurs and that pressure to depth ratios often decreases with uplift and underpressures have been observed in severely uplifted shales. This observation provides evidence that hydrocarbons have been expelled from the shales. Indeed, isotopic evidence indicates that much of the gas within shallow plays such as the Antrim shale has a biogenic origin ([Wen *et al.* 2015](#)). This has been interpreted to indicate that open fracture networks within these shallowly buried shales formed as a result of uplift and/or glacial loading/unloading and that this allowed thermogenic gas to escape but also allowed methanogenic bacteria to enter the shale resulting in biogenic methane production ([Wen *et al.* 2015](#)). However, it is also possible that these shales were never sufficiently mature to undergo thermogenic methane production and instead only ever contained biogenic methane. Irrespective of the mechanism, the fact that these plays remain underpressured suggests that groundwaters cannot access the open fracture networks indicating that self-sealing has occurred.

Dynamic data from shale plays

A few shallowly buried shales (e.g. Antrim shale) have produced small amounts of gas at economic rates without hydraulic fracturing probably due to the presence of natural fractures developed during uplift (e.g. [Apotria *et al.* 1994](#)). Deep shale resource plays have only been produced at economic rates when hydraulically fractured and injected with proppant to prevent the fractures from closing during clean-up and subsequent production ([King 2010](#)). Hydraulic fracture treatments in shale formations are performed in a multi-stage sequence in long horizontal wells, where between 15 000 to 70 000 m³ of fluid are injected. Each stage usually aims at simultaneously propagating several hydraulic fractures 10 to 30 m apart along the well, with an injection rate of 1.5 to 2 m³ min⁻¹ per fracture. Microseismic data suggests that hydraulic fractures are mainly contained within the producing shale despite such high injection volumes and rates ([Fisher and Warpinski 2012](#)).

Other studies (e.g. [Rickman *et al.* 2008](#); [Britt and Schoeffer 2009](#); [Buller *et al.* 2010](#)) have suggested that it is economically advantageous to focus hydraulic fracture treatments on the most brittle layers in shale plays rather than the more clay-rich intervals. It should, however, be noted that despite the common assertion that petroleum production rates are better from brittle shales there are few publications that provide evidence to support this strategy; notable exceptions being [Buller *et al.* \(2010\)](#) and [Salahshoor *et al.* \(2020\)](#). Hydraulic fractures in brittle shales may be more productive than in ductile shales for several reasons. Firstly, ductile shales tend to be more clay-rich than brittle shales and hence have lower permeability. Second, hydraulic fractures in clay-rich shales are prone to proppant embedment resulting in fracture closure.

After hydraulic fracture stimulation, production rates from shale plays fall rapidly (e.g. [Baihy *et al.* 2010](#)). For example, production

rates can fall by over 90% within the first year of production. It is tempting to conclude that this is due to closure of propped fractures. However, modelling indicates that the rapid fall in gas flow rates may simply be due to the rapid production of gas from the large volume of fresh surface area created during hydraulic fracturing ([Wang 2017](#)). The success of restricted-rate practice in enhancing gas production from some shale plays (e.g. the Haynesville) may be the result of the higher downhole pressures suppressing the closure of hydraulic fractures ([Zhao *et al.* 2021](#)). Also, refracturing wells by injecting into the original perforations can result in significant increases in productivity although it is not clear whether this is due to the reopening of closed hydraulic fractures or the creation of new fractures ([Asala *et al.* 2016](#)).

In summary, shale resource plays represented a brittle end-member to shale behaviour. Data obtained during the exploration, appraisal and production of shale resource plays suggests that: (i) economic rates of production are mostly not possible without placing proppant within hydraulic fractures, (ii) ductile/clay-rich shales do not produce at economic rates possibly due to fracture closure resulting from proppant embedment, (iii) despite shale plays having a low clay content and containing faults and fractures, shale resource plays have managed to retain abnormal fluid pressures, sometimes over very long periods.

Predicting the impact of shale-hosted faults and fractures on fluid flow

In general, those exploring for petroleum in conventional reservoirs take two broad approaches to predicting the risk of mechanical top seal leakage. The first, assesses whether faults and fractures are likely to have been recently formed or reactivated. The second, attempts to assess whether deformation is likely to have resulted in dilation. Those involved in the production of petroleum from shale resource plays tend to be more focused on predicting the likelihood that hydraulic fractures will remain open as pore pressures are reduced during production. The following section describes the different approaches used for predicting the formation of fractures and dilatant faults as well as the conditions required for them to remain conduits for the transmission of significant volumes of fluid.

Predicting fault and fracture formation and reactivation

The observation that maximum pore pressure often coincides with the minimum horizontal stress, S_{hmin} , has been interpreted to suggest that natural hydraulic fractures are formed when the pore pressure, P_p , exceeds the minimum horizontal stress allowing leakage to occur (e.g. [Gaarenstroom *et al.* 1993](#)). This led to the development of the retention capacity, RC , as an indicator of the likelihood of top seal failure ([Gaarenstroom *et al.* 1993](#)), where:

$$RC = S_{hmin} - P_p \quad (3)$$

Some authors argue that the tensile strength of the top seal needs to be taken into account when assessing the pore pressure at which it will leak (e.g. [Ingram and Urai 1999](#)). Another criticism of RC is that it does not take into account the phase (i.e. brine or petroleum) in which the pressure measurement has been taken. In particular, [Bjørkum *et al.* \(1998\)](#) argue that, in a water-wet system, high pressures in the petroleum phase does not increase the risk of natural hydraulic fractures forming because this is balanced by the interfacial tension between the wetting on non-wetting phases and is not transmitted to the rock. They argue that it is only overpressures in the wetting phase (brine) that increase the risk of hydraulic fractures forming. [Swarbrick *et al.* \(2010\)](#) argued that 'aquifer seal capacity' was an improvement on RC because it risks top seal failure based on the pressure within the wetting phase.

Another problem with RC is that it does not take into account the possibility that shear failure can cause leakage (Nordgård Bolås and Hermanrud 2003). Consequently, several other criteria have been developed that predict the likelihood that a top seal will experience shear failure. Morris *et al.* (1996) used slip tendency, ST , to predict shear failure, which is the ratio of shear stress, τ , to effective normal stress, σ'_n , acting on a fault plane, to assess the likelihood of slip on a cohesionless fault.

$$ST = \frac{\tau}{\sigma'_n} \quad (4)$$

Castillo *et al.* (2000) used the Coulomb fault function, CFF , which is the difference between the shear stress acting on a fault and the shear stress required to cause reactivation of a cohesionless fault:

$$CFF = \tau - \mu(\sigma_n - P_p) \quad (5)$$

where μ is the coefficient of friction of the fault.

Wiprut and Zoback (2002) developed the critical stress perturbation, CPP , which is the increase in pore pressure that would be required to decrease the effective normal stress on a cohesionless fault sufficiently to cause reactivation. Mildren *et al.* (2005) proposed the fault analysis seal technology, $FAST$, which is similar to CPP , but takes into account the fact that faults can have cohesion.

Conditions required for fault dilation

The metrics for assessing leakage risk described in the previous section are based on the likelihood that faults and fractures have been recently formed or reactivated. There is, however, a large volume of experimental data from the rock and soil mechanics literature that shows that faulting is not always accompanied by a permeability increase. For example, experiments on porous sandstones show that two end member modes of deformation may be distinguished based on the post-yield macroscopic structure of samples (e.g. Griggs and Handin 1960). The first, localized or brittle deformation, results in the formation of discrete slip planes, which accommodate most of the strain. The second, distributed or ductile deformation, does not result in the formation of discrete slip surfaces; instead strain is accommodated throughout the sample. A transitional regime, often referred to as the brittle-to-ductile transition, exists by which deformation occurs along multiple slip planes (Scott and Nielsen 1991). Localized deformation leads to dilation, which results in a permeability increase if the porosity is <15% at the time of faulting or a permeability decrease if the porosity is >15% (e.g. Zhu and Wong 1997). Sandstone deformed in a ductile manner or on the brittle-ductile transition experiences compaction and permeability reduction. Similar results have also been obtained from deformation experiments on clay-rich shales (Bolton *et al.* 1998; Gutierrez *et al.* 2000; Zhang and Rothfuchs 2004; Holland *et al.* 2006). For example, Holland *et al.* (2006) showed that the threshold pressure of clay-rich faults was higher than the undeformed sediment. Bolton *et al.* (1998) suggested that the shear deformation of normally consolidated shales was likely to result in a permeability decrease whereas faulting of overconsolidated shales was likely to result in permeability increase.

Several studies have attempted to assess the risk that faulting will result in the formation dilatant flow paths. For example, Ferrill *et al.* (2009) introduced the concept of dilation tendency, T_d , (equation 6) as a measure of whether the likelihood that a particular point on a fault will experience compaction or dilation. T_d as:-

$$T_d = \frac{\sigma_1 - \sigma_n}{\sigma_1 - \sigma_3} \quad (6)$$

Ferrill *et al.* (2020) provide several examples where calcite cement

occurs along fault segments with a high T_d whereas only slickenlines are present on sections with a low T_d .

Ingram *et al.* (1997) suggested that a useful indicator of the likely behaviour of mudrocks is the brittleness index, BRI , which is defined as:

$$BRI = \frac{UCS}{UCS_{NC}} \quad (7)$$

where UCS is the current unconfined compressive strength of the rock and UCS_{NC} is the unconfined compressive strength of rock with normal consolidation for the effective stress that the rock is presently experiencing. Ingram *et al.* (1997) suggest that rocks become brittle and are prone to leakage if BRI was greater than 2 at the time of faulting. UCS_{NC} can be estimated from empirical correlations found in the soil mechanics literature (Craig 1987) such as:

$$UCS_{NC} = 0.5\sigma' \quad (8)$$

where σ' is the *in situ* stress corresponding to normal consolidation at the depth of interest. UCS can be measured in the laboratory or estimated from logs. Ingram *et al.* (1997) suggested that UCS could also be estimated from compressional wave velocities using:

$$\log(UCS) = -6.36 + 2.45 \log(0.86V_p - 1172) \quad (9)$$

where UCS is in MPa and V_p is in m s^{-1} . Unfortunately, datasets have not been published to provide an indication of the accuracy to which BRI can be used to risk seal leakage.

Overconsolidation ratio, OCR , is the ratio of the maximum divided by the current effective stress, i.e.:

$$OCR = \frac{\sigma'_{\max}}{\sigma'_{\text{present}}} \quad (10)$$

OCR values measured in the laboratory can give considerably higher values than those calculated using equation (10) because processes such as cementation increase the stiffness of the rock and therefore increase the apparent maximum stress to which the rocks have been exposed. OCR has been used as a measure of whether faulting was likely to be compactional or dilatant. In particular, Nygård *et al.* (2006) suggested that heavily overconsolidated mudrocks ($OCR > 2.5$) are prone to deforming in a brittle manner and resulting in the formation of dilatant faults.

It should be emphasized that, although faulting of shale caprocks with high OCR values increases risk of leakage, there are a large number of productive, fill to spill, reservoirs in heavily faulted uplifted areas that are likely to be highly overconsolidated. For example, there have been several recent oil and gas discoveries in highly uplifted reservoirs with shale caprocks in the Barents Sea, offshore Norway (Table 2). It is possible that faults within these reservoirs have not recently reactivated or that any faults that experienced reactivation and leakage are not present at crest of the structures creating an underfilled reservoir (e.g. Edmundson *et al.* 2020). It is noteworthy that the most important seals for these reservoirs are the Hekkingen and Fuglen shales, which contain around 45 to 65% clay (Hansen *et al.* 2020; Paulsen *et al.* 2022). These have not reached temperatures of >80°C and therefore will not have been embrittled by mesodiagenetic alteration. In which case, it is possible that faults have reactivated but leakage was limited by self-sealing.

Controls on fault and fracture closure

Several studies have examined the controls on the closure of faults and fractures. For example, Bandis *et al.* (1983) indicated key controls including: (i) effective shear and normal stress (i.e. total shear and normal stress minus pore pressure); (ii) initial contact area; (iii) relative amplitude and distribution of apertures between fracture

Table 2. Shallow discoveries in the Barents Sea

Field	Well no.	Hydrocarbon type	Current depth (m TVDSS)	Uplift (m)	Maximum burial depth (m TVDSS)	OCR
Wisting Central	'7324/8-1	Oil	246	1500	1746	7.1
Hanssen	'7324/7-2	Oil	262	1800	2062	7.9
Isfjell	'7220/2-1	Gas	360	1000	1360	3.8
Caurus	'7222/11-1	Gas	264	1400	1664	6.3
Norvarg	'7225/3-1	Gas	307	1700	2007	6.5
Mercury	'7324/9-1	Gas	225	1600	1825	8.1
Pingvin	'7319/12-1	Gas	537	250	787	1.5

Modified from [Løkke-Sørensen et al. \(2017\)](#). Uplift was estimated using maps provided in [Henriksen et al. \(2011\)](#) and [Baig et al. \(2016, 2019\)](#).

walls; (iv) fracture wall roughness; (v) strength and deformability of asperities; and (vi) thickness, type and properties of any infilling material present. There are many models to calculate fracture closure ([Goodman 1974](#); [Bandis et al. 1983](#); [Alramahi and Sundberg 2012](#)) but these often contain terms, such as joint roughness coefficient, that are difficult to estimate ([Cho et al. 2013](#)).

Effective stress is a key parameter in models for both fracture permeability and fracture compliance (e.g. [Mckee et al. 1988](#); [Raghavan and Chin 2004](#)). The importance of effective stress on fracture closure is supported by numerous experimental studies conducted within the laboratory and in boreholes. For example, [Figure 7](#) shows that the permeability of a fractured sample of Whitby shale, which is analogous to shale caprocks in the North Sea, is reduced by around 5 orders of magnitude as effective normal stress is increased from 7.2 to 20.6 MPa. The impact of normal stress on fault closure is also confirmed by *in situ* packer tests. For example, [Figure 8](#) shows the results of a packer test conducted within a fault zone in the Opalinus clay and suggests that the hydraulic conductivity of the zone is reduced by around 5 orders of magnitude as effective normal stress is increased from 0 to 3 MPa.

The mechanical properties of the wall rock also have a significant impact on fracture closure. For example, [Cao et al. \(2016\)](#) showed that fracture conductivity was more stress-sensitive in rocks with low Young's modulus and high Poisson's ratio. The proppant embedment test is routinely conducted to assess how propped hydraulic fractures are likely to behave as effective stress is increased ([Katende et al. 2021](#)). These tests have shown that

proppant embedment, and hence fracture closure, tends to increase with increasing clay content. The impact of clay content on self-sealing was noted by [Bourg \(2015\)](#) who argued that shale containing <1/3 clay tended to be brittle whereas more clay-rich shales tended to behave in a ductile manner.

Clay content does not only impact mechanical-induced closure of fractures, it is also a significant control on shale swelling, which is widely recognized as an important, if not the most important, process responsible for the self-sealing of fractures (e.g. [Di Donna et al. 2022](#); [Zhang and Talandier 2023](#)). Shale swelling occurs over longer periods of time than the initial mechanical response and requires the presence of water. The requirement for water potentially means that shale swelling, and hence the self-sealing of faults and/or fractures could be retarded if flowing gases dehydrate the wall rock. The implications of such processes for effective barrier performance require further investigation.

Fault and fracture-related fluid flow: the importance of drive

The low compressibility of brine saturated rocks means that only a small proportion of the pore water (<1%) will be expelled from a 100% brine saturated compartment even if fluid pressures become sufficiently high to result in the formation of faults or fractures that connect to normally pressured strata ([Pedersen and Bjørlykke 1994](#); [Smalley et al. 2004](#)). For example, the amount of water expelled, V_{exp} , if the overpressure in layer B in [Figure 9](#) was sufficient to result

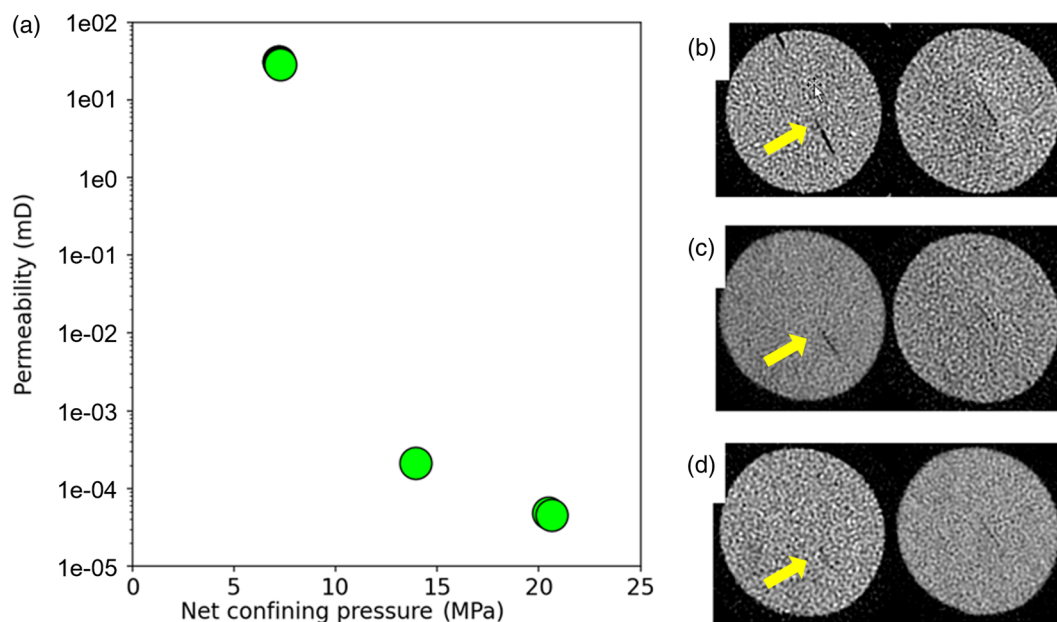


Fig. 7. Results from an experiment investigating the impact of confining pressure on a core plug of Whitby Shale containing a propped fracture (based on [Al-Hajri 2018](#)): (a) is a plot of permeability against confining pressure, (c) to (d) are CT scans through the sample at 7.2, 13.9 and 20.6 MPa respectively. Note how the fracture (arrow) has closed as confining pressure is increased.

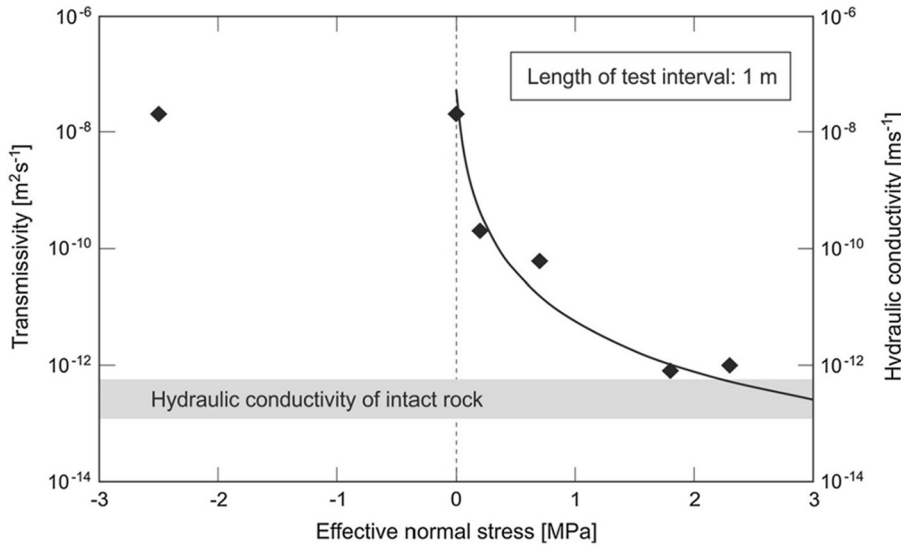


Fig. 8. Plot of effective normal stress v. hydraulic conductivity for a packer test conducted in a faulted interval of the Opalinus Clay (from [Marschall et al. 2017](#)).

in the formation of a fault/fracture that connected to layer A would be:

$$V_{\text{exp}} = \Delta P(C_w + C_p)V_B \quad (11)$$

where ΔP is the change in pressure, C_w is the brine compressibility, C_p is the pore volume compressibility and V_B is the pore volume within the sandstone in layer B. Assuming values of C_w and C_p of 4.3×10^{-10} and $\sim 4.3 \times 10^{-10}$ Pa respectively and a change in pressure of 3 MPa, which is equivalent to the difference in fracture opening and closure pressure shown in [Figure 9](#), the formation of a fault or fracture joining layers A and B would only result in the expulsion of pore water equivalent to 0.4% V_B .

The presence of active drive mechanisms could maintain fluid pressures above the fracture closure pressure and hence increase the volume of fluid focused along the fault. Three key drive mechanisms that operate in the subsurface are (i) recharge in a confined aquifer driven by the high relief of the topography ([Fig. 10a](#)); (ii) dewatering of compacting shales ([Fig. 10b](#)), and (iii) the presence of a buoyant hydrocarbon column ([Fig. 10c](#)). The former two mechanisms have considerable scope for concentrating flow along faults/fractures as the total volume is controlled by the amount of fluid entering the aquifer in the example shown in [Figure 10a](#) and the volume of fluid expelled from shales in the example shown in [Figure 10b](#). The volumes of fluid that could be focused through fault and fracture networks as a result of these processes will be dependent upon the specific situation and can vary widely. For example, [Giles \(1987\)](#) compiled a list of subsurface flow rates, which suggested that compaction driven flow could produce flow rates of 10^{-7} to 0.1 m/year with most values being

between 10^{-6} and 10^{-3} m/year. On the other hand, flow rates in aquifers varied between 10^{-2} and 10^4 m/year with most values between 0.1 and 30 m/year. Extreme focusing of flow, such as would occur if fluid flow through a 10 m thick aquifer was concentrated along a single fault/fracture could therefore produce fluxes of 10^{-5} to 10^{-2} m³/year per m length of fracture for the case of compactional flow and 1 to 300 m³/year per m length of fracture for aquifer flow. Although, [equation \(11\)](#) does not strictly apply to gas as its expansion is controlled by the Non-Ideal gas law, it does provide an indication as to the impact on leakage due to sediment containing a high gas saturation. In particular, based on the same geometry shown in [Figure 9](#) but with layer B having a 80% gas saturation, it is possible to exchange C_w with gas compressibility in [equation \(11\)](#) suggests that a change in pressure of 3 MPa would result in a loss of around 10% of the gas present.

Discussion: implications for selection of subsurface disposal sites

Clay-rich shales, particularly those that act as caprocks to petroleum reservoirs, often have such low permeability and high threshold pressures that faults and/fractures represent the key risk of leakage. This cannot, however, be taken for granted when choosing sites for disposal of waste materials in the subsurface that rely on shale barriers for safety. In other words, site selection will require assessment of the risk of leakage through shale matrix as well as faults/fractures; methodologies that can be used to assess these two issues are discussed separately below.

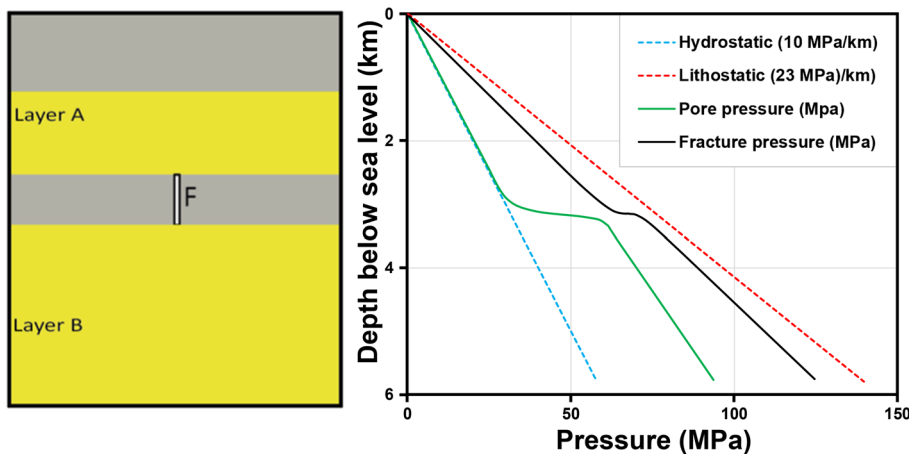


Fig. 9. Model of a normally pressured sandstone (layer A) separated from an overpressured sandstone (B) by a shale interval. A fracture (F) forms when the pressure in layer B reaches the fracture pressure.

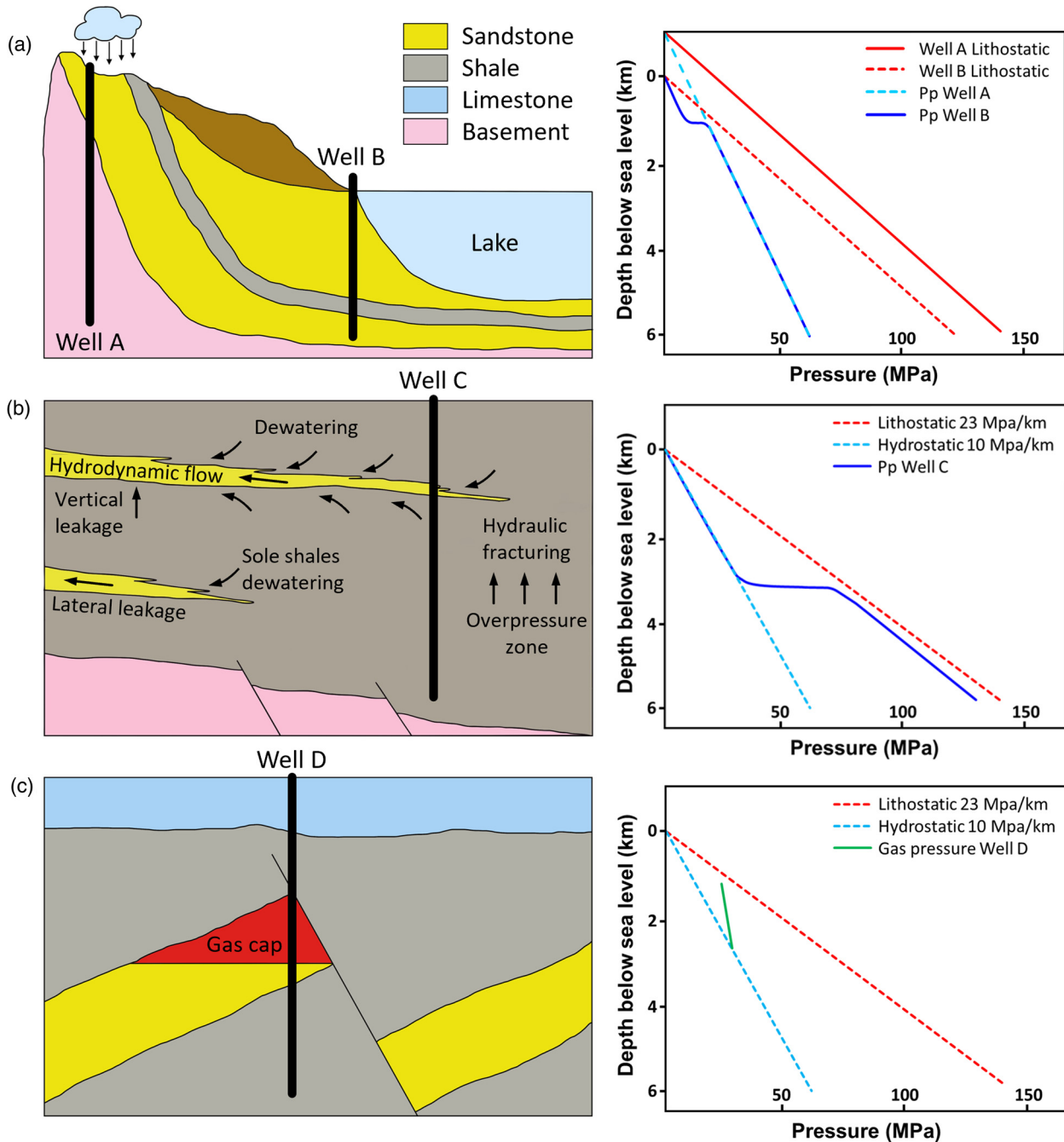


Fig. 10. Summary of key drive mechanisms that could in theory maintain overpressures that are sufficiently high to suppress self-sealing of dilatant faults and fractures in soft shales: (a) is recharge in a confined aquifer driven by the high relief of the topography; (b) dewatering of shales, and (c) the presence of a buoyant hydrocarbon column.

Assessment of risk of leakage through shale matrix

In some cases, such as storage of CO₂ in depleted petroleum reservoirs, there is strong geological evidence to suggest that leakage through the shale matrix is unlikely to be a significant risk on the timescales of required for waste disposal. However, in cases such as disposal of nuclear waste in shale and storage of CO₂ in saline aquifers sealed by shale caprocks, it is necessary to thoroughly characterize the matrix flow properties of shales that are being relied on to provide a barrier to fluid flow. Initial screening to identify a range of possible sites may be undertaken by examining outcrop analogues to ensure the presence of thick shale that does not contain obvious seal bypass structures such as sandstone stringers or sand injections (e.g. Cartwright *et al.* 2007). Once a small number of potential sites have been identified more detailed analysis of the

risk of leakage via the matrix is required and this will generally require drilling boreholes, conducting wire-line log analysis, packer experiments as well as analysing core and/or drill cuttings. The flow properties of core, such as permeability and capillary entry pressure should be obtained. It is important to conduct measurements at subsurface conditions as the flow properties of shale are sensitive to stress, pore pressure and fluid saturation. Great care should also be taken during handling, cutting and storing core as well as its saturation (e.g. Ewy 2015, 2018).

Analysis of natural tracers has also proven particularly useful for proving that leakage via the shale matrix is a low risk. For example, Koroleva *et al.* (2011) measured the oxygen and hydrogen isotopic composition, as well as the chloride content, of pore waters extracted from the Opalinus clay at the Mont Terri test site, Switzerland. The results strongly suggested that the profiles obtained were controlled

by diffusive exchange with the underlying Dogger aquifer starting between 2 and 4 Ma. In other words, Darcy flow into the Opalinus had not contributed significantly to element mobility.

Assessment of risk of fault and fracture-related leakage

Once the uncertainty associated with leakage through the matrix of a shale barrier has been minimized by the relevant analyses, it is necessary to assess the potential for leakage via faults and fractures. Evidence presented above indicates that faults through weak, clay-rich, shales may not act as significant conduits for fluid flow unless a mechanism is present to maintain overpressures at or above the minimum horizontal stress. Nevertheless, it is probably sensible to avoid sites that are cut by recently active, seismic-scale faults, particularly as they have been shown to act as temporary conduits to overpressured fluids and in areas subject to significant uplift and erosion. A range of methods can be used in such assessment including analysis of records of recent seismicity, field work to identify fault terraces formed by recent fault movement and the analysis of 3D seismic data. The latter could involve the use of some of the measures for quantifying the risk of fault reactivation and dilatancy as discussed above.

It is very difficult to predict the position of sub-seismic faults or whether an area will develop faults and/or fractures at a future date. It is, however, possible to choose disposal sites in areas where fault and fracture-related leakage would be extremely unlikely to create flow conduits and that any temporary flow conduits would rapidly self-seal. The data collected by the petroleum industry indicates that risk of leakage is minimized by choosing sites with shale barriers that have a high clay content (>40%) with a combination of low Young's modulus and high Poisson's ratio. Evidence also indicates that reservoirs with shale caprocks that have high overconsolidation ratios (>2.5) are at risk of leakage although many examples exist where caprocks with higher OCRs have retained petroleum columns. Evidence also suggests that leakage is concentrated along seismic-scale faults and therefore avoiding placing disposal sites close to such features is advised. This is probably not possible for CO₂ storage sites because by necessity they need to cover large areas but avoiding seismic-scale faults when siting disposal sites for nuclear waste is possible due to their relatively small footprint.

To apply lessons learned from the petroleum industry in the appraisal of subsurface disposal sites it is important to ensure that equivalent data are available so that comparisons are valid. Unfortunately, the type and quality of methods used to characterize the subsurface differ significantly not only between industries but also between different disciplines within a particular industry. The measurement of mechanical properties is a particularly good example. At one end of the spectrum, the nuclear waste disposal industry has conducted extremely rigorous long-term experiments

on the mechanical properties of shale. For example, creep experiments are often run for over a year (e.g. [Horseman *et al.* 2005](#)) for samples investigated by the nuclear waste industry. At the other end of the spectrum, the shale gas industry developed relatively quickly and therefore a pragmatic approach was taken in which far shorter experiments were undertaken. For example, it is common to conduct creep experiments that last for as little as 24 hours (e.g. [Sone and Zoback 2013](#)).

Wire-line log and mineralogical analysis are relatively standard techniques used by all industries involved with subsurface characterization and are therefore particularly useful for comparing different sites.

Indicators of the potential of faults and fractures to self-seal

Wire-line log data can be used to calculate dynamic elastic properties such as Young's modulus and Poisson's ratio. These are used extensively within the shale gas industry as an indicator of brittleness. To assess their potential use in the characterization of the barrier performance of shale in disposal or storage sites dynamic, Young's modulus and Poisson's ratio from a range of shale resource plays, top seals and host shales to potential deep nuclear waste repositories have been calculated and compared to a commonly used indicator of brittleness ([Fig. 11](#)). Overall, all of the shale resource plays have significant sections that plot in the brittle domain. Data from the Opalinus clay in an area appraised for a potential repository in Switzerland clearly plots in the ductile domain. Shale top seals generally also plot in the ductile domain but some horizons in the brittle domain probably reflecting the presence of carbonate cemented or quartz-rich layers.

The mineralogy of shale can be measured using a range of techniques including X-ray diffraction (XRD), infrared spectroscopy, as well as image analysis of back scattered electron images and mineral distributions generated from energy or wave dispersive X-ray spectrometry. The accuracy of XRD-derived measures of mineral content varies significantly depending upon the technique used but overall is probably the most accurate. We have therefore generated a database of XRD-derived bulk mineralogies from shale caprocks to petroleum reservoirs, shale resource plays and shale hosts to potential deep nuclear waste repositories. The results for the potential nuclear waste disposal facilities are plotted on a ternary diagram showing clay-carbonate-quartz and feldspar content ([Fig. 12](#)), which can be compared to the results for top seals and shale resource plays shown in [Figures 2 and 5](#) respectively. It is clear from the results that most of the host rocks for nuclear waste repositories and the top seals have >40% clay whereas most of the shale resource plays have <40% clay. There are clearly exceptions due, for example, to the presence of silty lamina within caprocks to petroleum reservoirs or clay-rich lamina in shale resource plays.

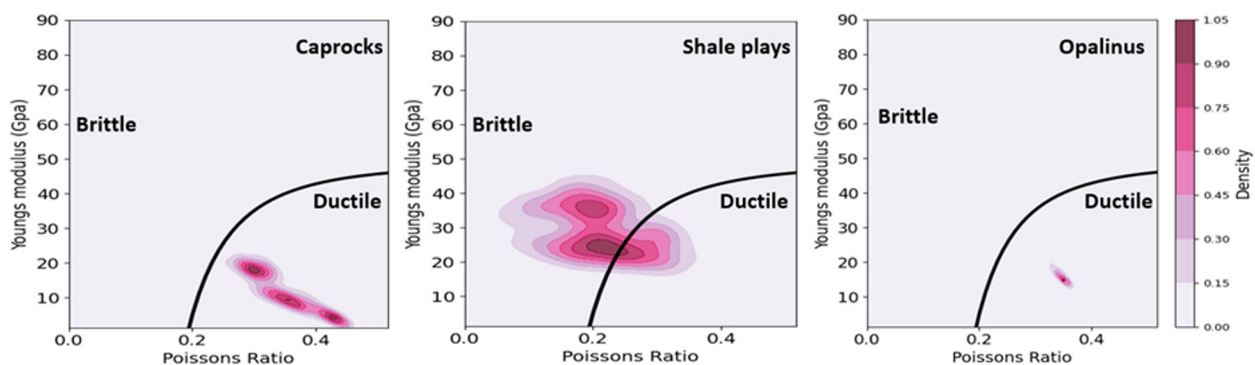


Fig. 11. Plot of dynamic Poisson's ratio against Young's modulus for (a) shale caprocks, (b) shale plays, and (c) deep geological repositories; the black line represents divides brittle to ductile behaviour according to [Grieser and Bray \(2007\)](#).

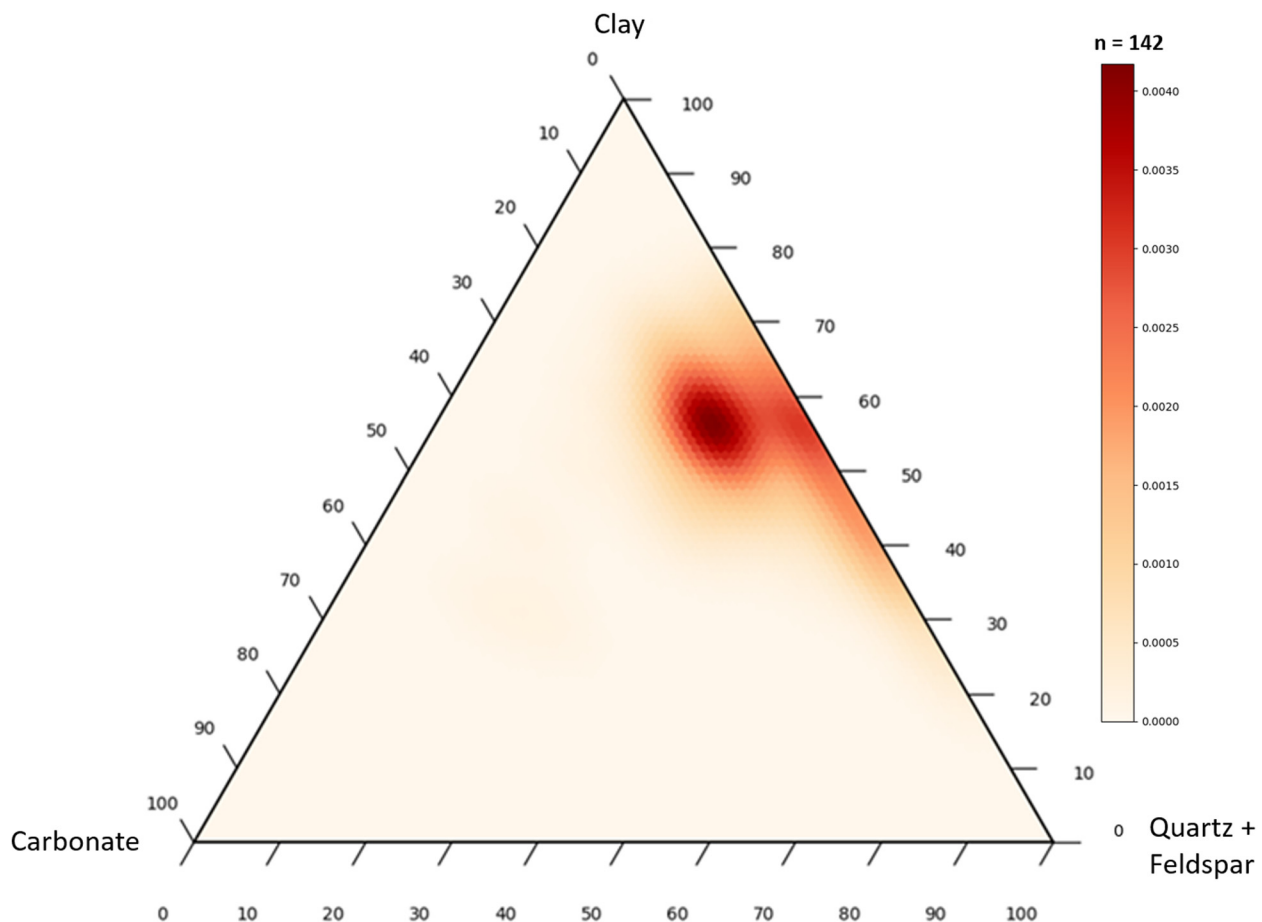


Fig. 12. Mineralogical composition from XRD of mudstone formations with potential to host a geological disposal facility of candidate radioactive waste sites. Data sourced from NAGRA and the NEA (2022). The scale is the probability density function (see Scott (1992)). It is a measure of the density of data within a given area of the ternary plot.

However, overall, clay content appears to be a robust indicator of the ability of a shale to act as a long-term barrier to fluid flow. A key caveat is that none of the examples provided have been from very low porosity clay-rich shale. It is quite feasible that clay-rich shales could also undergo embrittlement during deep diagenesis that would reduce the ability of any faults and fractures that are subsequently formed to self-seal.

Overpressure maintenance

Leakage along faults and fractures in clay-rich, low strength, shale is still possible if pore fluid pressures are maintained that are close to the S_{hmin} . Hydrogeological models based upon downhole pressure measurements can be used to estimate present-day groundwater flows and whether these are sufficient to maintain high overpressures. Clearly, it is vital to avoid placing a deep nuclear waste repository in a location where significant groundwater flow would be concentrated if impacted by future deformation. Gas is also generated as a result of the decay of nuclear waste and the metallic vessels in which it is likely to be contained, which could in theory lead to the generation of overpressures that are sufficient to cause faulting or hydraulic fracturing of the host shale. However, the volumes of gas generated from the decay of nuclear waste can be predicted and therefore the facilities can be designed to ensure that pressures never reach the levels required to induce dilatant faulting or fracturing. Also, by selecting a repository site within a clay-rich, low strength, shale ensures that any dilatant faults or fractures would rapidly self-seal in the unlikely event that they were produced as a result of either natural processes or high gas pressures generated in the repository.

Significant leakage from CO₂ storage sites is potentially more likely than groundwater flow through deep nuclear waste repositories due to the high volumes of (compressible) gas involved and the permeable nature of the reservoir, which would allow the rapid flow of gas to dilatant faults and fractures allowing pressures to be maintained above the closure pressure. The increased risk of CO₂ leakage is supported by the observation that gas appears to have been preferentially lost from reservoirs in parts of the Barents Sea that have experienced significant glaciation, uplift and erosion. Risks of leakage due to the formation of dilatant faults and fractures can clearly be reduced by limiting the maximum pressure at which the CO₂ is stored. Application of sophisticated coupled fluid flow-geomechanical modelling software can also be used to reduce leakage risk by estimating the maximum pressure at which it is safe to store CO₂ without the risk of forming or reactivating faults and fractures in the top seal.

Conclusions

Several technologies being developed to reduce greenhouse gas emissions will rely on shale acting as a highly effective barrier to fluid flow sometimes on timescales of up to 1 million years. Data gathered by the petroleum industry provides strong evidence that clay-rich shale can act as a secure barrier on the timescales of interest for the disposal of waste products in the subsurface. The preservation of petroleum traps and abnormally pressured compartments beneath shales prove conclusively that clay-rich shales are capable of acting as an effective barrier on timescales in excess of 10 Ma even when highly faulted. There is also evidence that leakage

can occur through clay-rich shales due to flow along faults and/or fractures. Shales that deform in a brittle dilatant manner when hydrostatically pressured pose a particularly high risk of leakage. These shales may be recognized by using simple index properties. For example, they are likely to have one of more of the following characteristics: (i) low clay contents (<40% clay), (ii) low Poisson's ratio/high Young's modulus, and (iii) overconsolidation ratios of >2.5. It should be noted that such shales can still act as effective barriers provided that they do not contain critically-stressed faults. For example, highly overconsolidated shales ($OCR > 5$) have been identified that have retained their barrier performance despite being shallowly buried (<1 km) and having experienced repeated loading and unloading as a result of recent glacial cycles.

Leakage along faults and/or fractures in normally pressured, clay-rich, shales that are normally or slightly overconsolidated ($OCR < 2$) is less of a risk because faulting occurs without forming flow conduits. Leakage can, however, occur along faults and/or fractures in these shales if pore pressures are close to, or exceed, the S_{hmin} . In such cases, the faults/fractures will self-seal once pore pressures are reduced as a result of leakage.

Assessing the long-term risk of leakage through clay-rich shales therefore requires an assessment of whether drive mechanisms exist that can maintain sufficiently high overpressures to prevent faults and fractures from self-sealing. In this respect, whether a shale is likely to be an effective barrier to prevent leakage from a nuclear waste repository can be achieved by ensuring that no mechanisms for overpressure generation are active and then designing the repository to ensure that the gas generated from the waste products does not reach the pressures necessary to allow fault and fracture-related fluid flow to occur. Assessing the risk of leakage through shale caprocks to CO_2 storage sites is potentially more complex due to the large volumes of highly compressible CO_2 present, which could provide the drive required to suppress the self-sealing of faults and/or fractures.

Acknowledgements NAGRA are thanked for providing data from the Opalinus clay in Switzerland.

Author contributions QF: conceptualization (lead), data curation (equal), formal analysis (lead), funding acquisition (lead), investigation (lead), methodology (lead), project administration (lead), software (lead), supervision (lead), writing – original draft (lead), writing – review & editing (lead); IK: conceptualization (supporting), data curation (equal), formal analysis (supporting), investigation (supporting), visualization (lead), writing – original draft (supporting), writing – review & editing (supporting); APS: data curation (equal), formal analysis (supporting), investigation (supporting), validation (supporting), writing – original draft (supporting), writing – review & editing (supporting)

Funding The authors wish to thank NERC for funding this research through the SHAPE-UK project (grant number NE/R017565/1), which forms Challenge 3 of the UKUH (Unconventional Hydrocarbons in the UK Energy System) programme.

Competing interests The authors declare the following financial interests/personal relationships which may be considered as potential competing interests: Quentin Fisher has received research grants from a large number of oil and gas companies to conduct research work on fault and top seal analysis for petroleum reservoirs and CO_2 storage sites. He is supervisor or a PhD project sponsored by nuclear waste services. He is also on the geoscience advisory board for Nagra. Ieva Kaminskate and Adriana del Pino Sanchez declare no known competing interests.

Data availability The datasets generated during and/or analysed during the current study are not publicly available due to confidentiality issues but are available from the corresponding author on reasonable request. Raw data on the experiments related to fracture closure can be provided as well as tables of mineralogy from caprocks and shale gas plays. Some data have also been included from consultancy projects. We have permission to use the data but locations are to remain confidential.

References

- Al-Hajri, H.S.A. 2018. Investigation of the controls of fluid flow through shale and their relation to its mechanical properties. PhD thesis, University of Leeds.
- Almon, W.R., Dawson, W.C., Ethridge, F.G., Rietsch, E., Sutton, S.J. and Castellblanco-Torres, B. 2005. Sedimentology and petrophysical character of Cretaceous marine shale sequences in foreland basins - potential seismic response issues. *AAPG Hedberg Series*, **2**, 215–235, <https://doi.org/10.1306/1060766H231>
- Alramahi, B. and Sundberg, M.I. 2012. Proppant embedment and conductivity of hydraulic fractures in shales. In: 46th US Rock Mechanics/Geomechanics Symposium, Chicago, Illinois, June 2012.
- Amann-Hildenbrand, A., Bertier, P., Busch, A. and Krooss, B.M. 2013. Experimental investigation of the sealing capacity of generic clay-rich caprocks. *International Journal of Greenhouse Gas Control*, **19**, 620–641, <https://doi.org/10.1016/j.ijggc.2013.01.040>
- Andra 2009. *Rapport Mi-Parcours Pour Le Groupement de Laboratoires Transfert de Gaz*. Andra Dossier 2009. **C.RP.ASCM.09.0002/C**.
- Apotria, T., Kaiser, C.J. and Cain, B.A. 1994. Fracturing and Stress history of the Devonian Antrim shale, Michigan basin. In: 1st North American Rock Mechanics Symposium, NARMS, Austin, Texas, June 1994.
- Asala, H.I., Ahmadi, M. and Taleghani, A.D. 2016. Why re-fracturing works and under what conditions. *SPE Annual Technical Conference and Exhibition, Dubai, UAE, September 2016*, <https://doi.org/10.2118/181516-MS>
- Baig, I., Faleide, J.I., Jahren, J. and Mondol, N.H. 2016. Cenozoic exhumation on the southwestern Barents Shelf: estimates and uncertainties constrained from compaction and thermal maturity analyses. *Marine and Petroleum Geology*, **73**, <https://doi.org/10.1016/j.marpetgeo.2016.02.024>
- Baig, I., Faleide, J.I., Mondol, N.H. and Jahren, J. 2019. Burial and exhumation history controls on shale compaction and thermal maturity along the Norwegian North Sea basin margin areas. *Marine and Petroleum Geology*, **104**, <https://doi.org/10.1016/j.marpetgeo.2019.03.010>
- Baihly, J., Altman, R., Malpani, R. and Luo, F. 2010. Shale gas production decline trend comparison over time and basins. In: Proceedings - SPE Annual Technical Conference and Exhibition, Florence, Italy, September 2010, <https://doi.org/10.2118/135555-ms>
- Bandis, S.C., Lumsden, A.C. and Barton, N.R. 1983. Fundamentals of rock joint deformation. *International Journal of Rock Mechanics and Mining Sciences & Geomechanics Abstracts*, **20**, 249–268, [https://doi.org/10.1016/0148-9062\(83\)90595-8](https://doi.org/10.1016/0148-9062(83)90595-8)
- Birchall, T., Senger, K., Hornum, M.T., Olaussen, S. and Braathen, A. 2020. Underpressure in the northern Barents shelf: causes and implications for hydrocarbon exploration. *AAPG Bulletin*, **104**, 2267–2295, <https://doi.org/10.1306/02272019146>
- Birchall, T., Senger, K. and Swarbrick, R. 2022. Naturally occurring underpressure – a global review. *Petroleum Geoscience*, **28**, petgeo2021-051, <https://doi.org/10.1144/petgeo2021-051>
- Bjorkum, P.A., Walderhaug, O. and Nadeau, P.H. 1998. Physical constraints on hydrocarbon leakage and trapping revisited. *Petroleum Geoscience*, **4**, 237–239, <https://doi.org/10.1144/petgeo.4.3.237>
- Blatt, H. 1982. *Sedimentary Petrology*. W.H. Freeman and Company, New York.
- Bolton, A.J., Maltman, A.J. and Clennell, M.B. 1998. The importance of overpressure timing and permeability evolution in fine-grained sediments undergoing shear. *Journal of Structural Geology*, **20**, 1013–1022, [https://doi.org/10.1016/S0191-8141\(98\)00030-3](https://doi.org/10.1016/S0191-8141(98)00030-3)
- Bossart, P., Burrus, F., Jaeggi, D. and Nussbaum, C. 2017. The Mont Terri rock laboratory. In: *Rock Mechanics and Engineering Volume 2*, CRC Press, 469–510.
- Boulin, P.F., Bretonnier, P., Gland, N. and Lombard, J.M. 2012. Contribution of the steady state method to water permeability measurement in very low permeability porous media. *Oil & Gas Science and Technology – Revue d'IFP Energies Nouvelles*, **67**, <https://doi.org/10.2516/ogst/2011169>
- Bourdet, J., Kempton, R.H., Dyja-Person, V., Pironon, J., Gong, S. and Ross, A.S. 2020. Constraining the timing and evolution of hydrocarbon migration in the Bight Basin. *Marine and Petroleum Geology*, **114**, <https://doi.org/10.1016/j.marpetgeo.2019.104193>
- Bourg, I.C. 2015. Sealing Shales versus brittle shales: a sharp threshold in the material properties and energy technology uses of fine-grained sedimentary rocks. *Environmental Science and Technology Letters*, **2**, <https://doi.org/10.1021/acs.estlett.5b00233>
- Bowers, G.L. 1995. Pore pressure estimation from velocity data: accounting for overpressure mechanisms besides undercompaction. *SPE Drilling & Completion*, **10**, 89–95, <https://doi.org/10.2118/27488-pa>
- Bowker, K.A. 2007. Recent developments of the Barnett Shale play, Fort Worth Basin. *West Texas Geological Society Bulletin*, Search and Discovery Article #10126, **42**.
- Braathen, A., Bælum, K. et al. 2012. The Longyearbyen CO_2 Lab of Svalbard, Norway—initial assessment of the geological conditions for CO_2 sequestration. *Norwegian Journal of Geology*, **92**, 353–376.
- Brennwald, M.S. and van Dorp, F. 2009. Radiological risk assessment and biosphere modelling for radioactive waste disposal in Switzerland. *Journal of Environmental Radioactivity*, **100**, <https://doi.org/10.1016/j.jenvrad.2009.05.006>
- Britt, L.K. and Schoeffler, J. 2009. The geomechanics of a shale play: what makes a shale prospective? In: SPE Eastern Regional Meeting, Charleston, West Virginia, USA, September 2009, <https://doi.org/10.2118/125525-ms>

- Buller, D., Hughes, S., Market, J., Petre, E., Spain, D. and Odumosu, T. 2010. Petrophysical evaluation for enhancing hydraulic stimulation in horizontal shale gas wells. In: *Proceedings - SPE Annual Technical Conference and Exhibition*, Florence, Italy, September 2010, <https://doi.org/10.2118/132990-ms>
- Camp, W.K., Egenhoff, S., Schieber, J. and Slatt, R.M. 2016. A compositional classification for grain assemblages in fine-grained sediments and sedimentary rocks discussion. *Journal of Sedimentary Research*, **86**, <https://doi.org/10.2110/jsr.2015.100>
- Cao, H.T., Yi, X.Y., Lu, Y. and Xiao, Y. 2016. A fractal analysis of fracture conductivity considering the effects of closure stress. *Journal of Natural Gas Science and Engineering*, **32**, <https://doi.org/10.1016/j.jngse.2016.04.022>
- Cartwright, J., Huuse, M. and Aplin, A. 2007. Seal bypass systems. *American Association of Petroleum Geologists Bulletin*, **91**, <https://doi.org/10.1306/04090705181>
- Castillo, D.A., Bishop, D.J., Donaldson, I., Kuek, D., de Ruig, M., Trupp, M. and Shuster, M.W. 2000. Trap integrity in the Lam In Aria High-Nancarrow Trough region, Timor Sea: prediction of fault seal failure using well-constrained stress tensors and fault surfaces interpreted from 3D seismic. *The APPEA Journal*, **40**, <https://doi.org/10.1071/aj99009>
- Chalmers, G.R.L. and Bustin, R.M. 2012. Geological evaluation of Halfway-Doig-Montney hybrid gas shale-tight gas reservoir, northeastern British Columbia. *Marine and Petroleum Geology*, **38**, <https://doi.org/10.1016/j.marpetgeo.2012.08.004>
- Cho, Y., Apaydin, O.G. and Ozkan, E. 2013. Pressure-dependent natural-fracture permeability in shale and its effect on shale-gas well production. *SPE Reservoir Evaluation and Engineering*, **16**, 216–228, <https://doi.org/10.2118/159801-PA>
- Craig, R.F. 1987. *Soil Mechanics*. 4th edn. Van Nostrand Reinhold (UK), 410 pp.
- Crysdale, B. and Barker, C. 1990. Thermal and fluid migration history in the Niobrara Formation, Berthoud oil field, Denver Basin, Colorado. In: Nuccio, V.F., Barker, C.E. and Dyson, S.J. (eds) *Applications of Thermal Maturity Studies to Energy Exploration: U.S. Geological Survey Monograph*. Rocky Mountain Section (SEPM), 153–160.
- Delage, P. and Lefebvre, G. 1984. Study of the structure of a sensitive Champlain clay and of its evolution during consolidation. *Canadian Geotechnical Journal*, **21**, 21–35, <https://doi.org/10.1139/t84-003>
- Dickinson, G. 1953. Geological aspects of abnormal reservoir pressures in Gulf Coast Louisiana. *AAPG Bulletin*, **37**, 410–432, <https://doi.org/10.1306/5CEADC6B-16BB-11D7-8645000102C1865D>
- Di Donna, A., Charrier, P., Dijkstra, J., Andò, E. and Bésuelle, P. 2022. The contribution of swelling to self-sealing of claystone studied through x-ray tomography. *Physics and Chemistry of the Earth*, **127**, <https://doi.org/10.1016/j.pce.2022.103191>
- Doré, A.G., Scotchman, I.C. and Corcoran, D. 2000. Cenozoic exhumation and prediction of the hydrocarbon system on the NW European margin. *Journal of Geochemical Exploration*, **69–70**, 615–618, [https://doi.org/10.1016/S0375-6742\(00\)00137-0](https://doi.org/10.1016/S0375-6742(00)00137-0)
- Edmundson, I., Rotevatn, A., Davies, R., Yielding, G. and Broberg, K. 2020. Key controls on hydrocarbon retention and leakage from structural traps in the Hammerfest Basin, SW Barents Sea: implications for prospect analysis and risk assessment. *Petroleum Geoscience*, **26**, 589–606, <https://doi.org/10.1144/petgeo.2019-094>
- Eggbowaye, E.I. 2016a. Sedimentology and ichnology of upper Montney Formation tight gas reservoir, Northeastern British Columbia, Western Canada Sedimentary Basin. *International Journal of Geosciences*, **07**, <https://doi.org/10.4236/ijg.2016.712099>
- Eggbowaye, E.I. 2016b. Whole-rock geochemistry and mineralogy of Triassic Montney Formation, Northeastern British Columbia, Western Canada Sedimentary Basin. *International Journal of Geosciences*, **07**, <https://doi.org/10.4236/ijg.2016.71008>
- Engelder, T. and Fischer, M.P. 1994. Influence of poroelastic behaviour on the magnitude of minimum horizontal stress, S_h , in overpressured parts of sedimentary basins. *Geology*, **22**, 949–952, [https://doi.org/10.1130/0091-7613\(1994\)022<0949:JOPBOT>2.3.CO;2](https://doi.org/10.1130/0091-7613(1994)022<0949:JOPBOT>2.3.CO;2)
- Engelder, T. and Leftwich, J.T. 1997. A pore-pressure limit in overpressured South Texas oil and gas fields. *AAPG Memoir*, **67**, 255–267, <https://doi.org/10.1306/m67611c15>
- Evans, M.A. 1995. Fluid inclusions in veins from the Middle Devonian shales: a record of deformation conditions and fluid evolution in the Appalachian Plateau. *Geological Society of America Bulletin*, **107**, 327–339, [https://doi.org/10.1130/0016-7606\(1995\)107<0327:FIIVFT>2.3.CO;2](https://doi.org/10.1130/0016-7606(1995)107<0327:FIIVFT>2.3.CO;2)
- Ewy, R.T. 2015. Shale/claystone response to air and liquid exposure, and implications for handling, sampling and testing. *International Journal of Rock Mechanics and Mining Sciences*, **80**, <https://doi.org/10.1016/j.ijrmms.2015.10.009>
- Ewy, R.T. 2018. Practical approaches for addressing shale testing challenges associated with permeability, capillarity and brine interactions. *Geomechanics for Energy and the Environment*, **14**, <https://doi.org/10.1016/j.gete.2018.01.001>
- Ferrill, D.A., Morris, A.P. and McGinnis, R.N. 2009. Crossing conjugate normal faults in field exposures and seismic data. *AAPG Bulletin*, **93**, <https://doi.org/10.1306/06250909039>
- Ferrill, D.A., Smart, K.J. and Morris, A.P. 2020. Fault failure modes, deformation mechanisms, dilation tendency, slip tendency, and conduits v. seals. *Geological Society, London, Special Publications*, **496**, 75–98, <https://doi.org/10.1144/SP496-2019-7>
- Fisher, K. and Warpinski, N. 2012. Hydraulic-fracture-height growth: real data. *SPE Production and Operations*, **27**, 8–19, <https://doi.org/10.2118/145949-pa>
- Fisher, Q., Lorinczi, P. *et al.* 2017. Laboratory characterization of the porosity and permeability of gas shales using the crushed shale method: insights from experiments and numerical modelling. *Marine and Petroleum Geology*, **86**, <https://doi.org/10.1016/j.marpetgeo.2017.05.027>
- Fishman, N.S., Hackley, P.C., Lowers, H.A., Hill, R.J., Egenhoff, S.O., Eberl, D.D. and Blum, A.E. 2012. The nature of porosity in organic-rich mudstones of the Upper Jurassic Kimmeridge Clay Formation, North Sea, offshore United Kingdom. *International Journal of Coal Geology*, **103**, <https://doi.org/10.1016/j.coal.2012.07.012>
- Freeman, C.M., Moridis, G.J. and Blasingame, T.A. 2011. A numerical study of microscale flow behavior in tight gas and shale gas reservoir systems. *Transport in Porous Media*, **90**, <https://doi.org/10.1007/s11242-011-9761-6>
- Friedrich, M. and Monson, G. 2013. Two practical methods to determine pore pressure regimes in the Spraberry and Wolfcamp Formations in the Midland Basin. In: *Unconventional Resources Technology Conference*, 12–14 August 2013, Denver, Colorado, 2475–2486, <https://doi.org/10.1190/urtec2013-258>
- Furre, A.K., Eiken, O., Alnes, H., Vevatne, J.N. and Kier, A.F. 2017. 20 years of monitoring CO₂-injection at Sleipner. *Energy Procedia*, **114**, 3916–3926, <https://doi.org/10.1016/j.egypro.2017.03.1523>
- Gaarenstroom, L., Tromp, R.A.J., De Jong, M.C. and Brandenburg, A.M. 1993. Overpressures in the Central North Sea: implications for trap integrity and drilling safety. *Geological Society, London, Petroleum Geology Conference Series*, **4**, 1305–1313, <https://doi.org/10.1144/0041305>
- Gale, J.F.W., Laubach, S.E., Olson, J.E. and Fall, A. 2014. Natural fractures in shale: a review and new observations. *American Association of Petroleum Geologists Bulletin*, **98**, 2165–2216, <https://doi.org/10.1306/08121413151>
- Giles, M.R. 1987. Mass transfer and problems of secondary porosity creation in deeply buried hydrocarbon reservoirs. *Marine and Petroleum Geology*, **4**, 188–204, [https://doi.org/10.1016/0264-8172\(87\)90044-4](https://doi.org/10.1016/0264-8172(87)90044-4)
- Goodman, R.E. 1974. The Mechanical properties of joints. In: *Proc 3rd Int Congr International Society of Rock Mechanics*, Denver, 127–140.
- Goult, N.R., Sargent, C., Andras, P. and Aplin, A.C. 2016. Compaction of diagenetically altered mudstones – Part 1: mechanical and chemical contributions. *Marine and Petroleum Geology*, **77**, <https://doi.org/10.1016/j.marpetgeo.2016.07.015>
- Grieser, B. and Bray, J. 2007. Identification of production potential in unconventional reservoirs. In: *Society of Petroleum Engineers - Production and Operations Symposium*, Oklahoma City, Oklahoma, U.S.A., March 2007, <https://doi.org/10.2118/106623-MS>
- Griggs, D. and Handin, J. 1960. Observations on fracture and a hypothesis of earthquakes. *Geological Society of America Memoirs*, **79**, 347–364, <https://doi.org/10.1130/MEM79-p347>
- Grunau, H.R. 1987. A worldwide look at the cap-rock problem. *Journal of Petroleum Geology*, **10**, 245–265, <https://doi.org/10.1111/j.1747-5457.1987.tb00945.x>
- Guggenheim, S. and Martin, R.T. 1995. Definition of clay and clay mineral: joint report of the AIPEA nomenclature and CMS nomenclature committees. *Clays and Clay Minerals*, **43**, 255–256, <https://doi.org/10.1346/CCMN.1995.0430213>
- Gutierrez, M., Øino, L.E. and Nygård, R. 2000. Stress-dependent permeability of a de-mineralised fracture in shale. *Marine and Petroleum Geology*, **17**, [https://doi.org/10.1016/S0264-8172\(00\)00027-1](https://doi.org/10.1016/S0264-8172(00)00027-1)
- Hansen, J.A., Mondol, N.H., Tsikalas, F. and Faleide, J.I. 2020. Caprock characterization of Upper Jurassic organic-rich shales using acoustic properties, Norwegian Continental Shelf. *Marine and Petroleum Geology*, **121**, <https://doi.org/10.1016/j.marpetgeo.2020.104603>
- Heij, G. 2018. *Magnetic Fabrics and Paleomagnetism of North American Mudrocks: Relics of Complex Burial Histories*. PhD thesis, University of Oklahoma.
- Henriksen, E., Bjørnseth, H.M. *et al.* 2011. Chapter 17: Uplift and erosion of the greater Barents Sea: impact on prospectivity and petroleum systems. *Geological Society, London, Memoirs*, **35**, 271–281, <https://doi.org/10.1144/M35.17>
- Hildenbrand, A. and Urai, J.L. 2003. Investigation of the morphology of pore space in mudstones-first results. *Marine and Petroleum Geology*, **20**, <https://doi.org/10.1016/j.marpetgeo.2003.07.001>
- Hillis, R.R. 2001. Coupled changes in pore pressure and stress in oil fields and sedimentary basins. *Petroleum Geoscience*, **7**, 419–425, <https://doi.org/10.1144/petgeo.7.4.419>
- Holland, M., Urai, J.L., van der Zee, W., Stanjek, H. and Konstanty, J. 2006. Fault gouge evolution in highly overconsolidated claystones. *Journal of Structural Geology*, **28**, <https://doi.org/10.1016/j.jsg.2005.10.005>
- Horseman, S.T. 1994. *The Disposal of High Level Radioactive Waste in Argillaceous Host Rocks Identification of Parameters, Constraints and Geological Assessment Priorities*. No. ENRESA-04/94.
- Horseman, S.T., Higgo, J.J.W., Alexander, J. and Harrington, J.F. 1996. *Water, Gas and Solute Movement Through Argillaceous Media*. Nuclear Energy Agency Report CC-91/1 OECD.
- Horseman, S.T., Harrington, J.F., Birchall, D.J., Noy, D.J. and Cuss, R.J. 2005. *Consolidation and Rebound Properties of Opalinus Clay: A Long-Term, Fully-Drained Test*. British Geological Survey Technical Report CR05/128.

- Horsrud, P., Sønsteby, Ø.E.F. and Bøe, R. 1998. Mechanical and petrophysical properties of North Sea shales. *International Journal of Rock Mechanics and Mining Sciences*, **35**, 1009–1020, [https://doi.org/10.1016/S0148-9062\(98\)00162-4](https://doi.org/10.1016/S0148-9062(98)00162-4)
- Huggett, J.M. 2005. Clay Minerals. In: Shelley, R.C., Cocks, L.R.M., and Plimer, I.R. (eds) *Encyclopedia of Geology*, pp. 358–365.
- Hupp, B.N. and Donovan, J.J. 2018. Quantitative mineralogy for facies definition in the Marcellus Shale (Appalachian Basin, USA) using XRD-XRF integration. *Sedimentary Geology*, **371**, <https://doi.org/10.1016/j.sedgeo.2018.04.007>
- Ilgen, A.G., Heath, J.E. et al. 2017. Shales at all scales: exploring coupled processes in mudrocks. *Earth-Science Reviews*, **166**, <https://doi.org/10.1016/j.earscirev.2016.12.013>
- Ingram, G.M. and Urai, J.L. 1999. Top-seal leakage through faults and fractures: the role of mudrock properties. *Geological Society, London, Special Publications*, **158**, 125–135, <https://doi.org/10.1144/GSL.SP.1999.158.01.10>
- Ingram, G.M., Urai, J.L. and Naylor, M.A. 1997. Sealing processes and top seal assessment. *Norwegian Petroleum Society Special Publications*, **7**, 165–174, [https://doi.org/10.1016/S0928-8937\(97\)80014-8](https://doi.org/10.1016/S0928-8937(97)80014-8)
- Ito, D., Akaku, K., Okabe, T., Takahashi, T. and Tsuji, T. 2011. Measurement of threshold capillary pressure for seal rocks using the step-by-step approach and the residual pressure approach. *Energy Procedia*, **4**, 5211–5218, <https://doi.org/10.1016/j.egypro.2011.02.499>
- Jackson, W.A., Hampson, G.J. et al. 2022. A screening assessment of the impact of sedimentological heterogeneity on CO₂ migration and stratigraphic-baffling potential: Johansen and Cook formations, Northern Lights project, offshore Norway. *International Journal of Greenhouse Gas Control*, **120**, <https://doi.org/10.1016/j.ijggc.2022.103762>
- Jarvie, D.M., Hill, R.J., Ruble, T.E. and Pollastro, R.M. 2007. Unconventional shale-gas systems: the Mississippian Barnett Shale of north-central Texas as one model for thermogenic shale-gas assessment. *American Association of Petroleum Geologists Bulletin*, **91**, <https://doi.org/10.1306/12190606068>
- Kalani, M., Jähren, J., Mondol, N.H. and Faleide, J.I. 2015. Petrophysical implications of source rock microfracturing. *International Journal of Coal Geology*, **143**, <https://doi.org/10.1016/j.coal.2015.03.009>
- Karlsen, D.A. and Skeie, J.E. 2006. Petroleum migration, faults and overpressure, part I: calibrating basin modelling using petroleum in traps - a review. *Journal of Petroleum Geology*, **29**, <https://doi.org/10.1111/j.1747-5457.2006.00227.x>
- Katahara, K.W. and Corrigan, J.D. 2004. Effect of gas on poroelastic response to burial or erosion. *AAPG Memoir*, **76**, <https://doi.org/10.1306/m76870c7>
- Katende, A., O'Connell, L., Rich, A., Rutqvist, J. and Radonjic, M. 2021. A comprehensive review of proppant embedment in shale reservoirs: experimentation, modeling and future prospects. *Journal of Natural Gas Science and Engineering*, **95**, <https://doi.org/10.1016/j.jngse.2021.104143>
- Katz, A.J. and Thompson, A.H. 1986. Quantitative prediction of permeability in porous rock. *Physical Review B*, **34**, 8179, <https://doi.org/10.1103/PhysRevB.34.8179>
- Katz, A.J. and Thompson, A.H. 1987. Prediction of rock electrical conductivity from mercury injection measurements. *Journal of Geophysical Research*, **92**, 599–607, <https://doi.org/10.1029/JB092iB01p00599>
- King, G.E. 2010. Thirty years of gas shale fracturing: what have we learned? *Proceedings - SPE Annual Technical Conference and Exhibition*, Florence, Italy, September 2010, <https://doi.org/10.2118/133456-ms>
- Kishankov, A., Serov, P. et al. 2022. Hydrocarbon leakage driven by Quaternary glaciations in the Barents Sea based on 2D basin and petroleum system modeling. *Marine and Petroleum Geology*, **138**, <https://doi.org/10.1016/j.marpetgeo.2022.105557>
- Koroleva, M., Alt-Epping, P. and Mazurek, M. 2011. Large-scale tracer profiles in a deep claystone formation (Opalinus Clay at Mont Russell, Switzerland): implications for solute transport processes and transport properties of the rock. *Chemical Geology*, **280**, <https://doi.org/10.1016/j.chemgeo.2010.11.016>
- Kwon, O., Kronenberg, A.K., Gangi, A.F., Johnson, B. and Herbert, B.E. 2004. Permeability of illite-bearing shale: 1. Anisotropy and effects of clay content and loading. *Journal of Geophysical Research: Solid Earth*, **109**, <https://doi.org/10.1029/2004JB003052>
- Lamb, J. 2014. *An Examination of the Arkoma Foreland Basin and Its Petroleum System through Burial and Thermal History Modeling*. MSc thesis, University of Houston.
- Lazar, O.R., Bohacs, K.M., Macquaker, J.H.S., Schieber, J. and Demko, T.M. 2015. Capturing key attributes of fine-grained sedimentary rocks in outcrops, cores, and thin sections: nomenclature and description guidelines. *Journal of Sedimentary Research*, **85**, <https://doi.org/10.2110/jsr.2015.11>
- Lin, W. 1978. Measuring the permeability of Eleana argillite from area 17, Nevada Test Site, using the transient method.
- Lindeberg, E., Vuillaume, J.F. and Ghaderi, A. 2009. Determination of the CO₂ storage capacity of the Utsira formation. *Energy Procedia*, **1**, 2777–2784, <https://doi.org/10.1016/j.egypro.2009.02.049>
- Løkke-Sørensen, T., Oskarsen, T.T., Paknejad, A., Aadnøy, B., Sangesland, S. and Johansen, S.E. 2017. *Shallow Reservoirs in the Barents Sea*. Report for the Norwegian Petroleum Safety Authority.
- Longmuir, G. 2004. Pre-darcy flow: a missing piece of the improved oil recovery puzzle? *Proceedings - SPE Symposium on Improved Oil Recovery*, Tulsa, Oklahoma, April 2004, <https://doi.org/10.2523/89433-ms>
- Løseth, H., Gading, M. and Wensaas, L. 2009. Hydrocarbon leakage interpreted on seismic data. *Marine and Petroleum Geology*, **26**, <https://doi.org/10.1016/j.marpetgeo.2008.09.008>
- Losh, S. 1998. Oil migration in a major growth fault: structural analysis of the Pathfinder Core, south Eugene Island block 330, offshore Louisiana. *AAPG Bulletin*, **82**, 1694–1710.
- Losh, S., Walter, L., Meulbroeck, P., Martini, A., Cathles, L. and Whelan, J. 2002. Reservoir fluids and their migration into the South Eugene Island Block 330 reservoirs, offshore Louisiana. *AAPG Bulletin*, **86**, <https://doi.org/10.1306/61eeddce-173e-11d7-8645000102c1865d>
- Lu, J. 2008. *CO₂ Interaction with Aquifer and Seal on Geological Timescales: The Miller Oilfield, UK North Sea*. PhD thesis, University of Edinburgh.
- Macgregor, D.S. 1996. Factors controlling the destruction or preservation of giant light oilfields. *Petroleum Geoscience*, **2**, 197–217, <https://doi.org/10.1144/petgeo.2.3.197>
- Marschall, P., Giger, S. et al. 2017. Hydro-mechanical evolution of the EDZ as transport path for radionuclides and gas: insights from the Mont Terri rock laboratory (Switzerland). *Swiss Journal of Geosciences*, **110**, <https://doi.org/10.1007/s00015-016-0246-z>
- McKee, C.R., Bumb, A.C. and Koenig, R.A. 1988. Stress-dependent permeability and porosity of coal and other geologic formations. *SPE Formation Evaluation*, **3**, 81–91, <https://doi.org/10.2118/12858-PA>
- Mildren, S.D., Hillis, R.R., Lyon, P.J., Meyer, J.J., Dewhurst, D.N. and Boulton, P.J. 2005. FAST: a new technique for geomechanical assessment of the risk of reactivation-related breach of fault seals. In: Boulton, P. and Kaldi, J. (eds) *Evaluating Fault and Cap Rock Seals. AAPG Hedberg Series*, **2**, 73–85.
- Milicic, R.C. and Swezey, C.S. 2014. *Assessment of Appalachian Basin oil and Gas Resources: Devonian Gas Shales of the Devonian Shale-Middle and Upper Paleozoic Total Petroleum System*. USGS Professional Paper, **1708**.
- Miller, R.G. 1992. The global oil system: the relationship between oil generation, loss, half-life, and the world crude oil resource. *American Association of Petroleum Geologists Bulletin*, **76**, 900–902, <https://doi.org/10.1306/bdff8d9e-1718-11d7-8645000102c1865d>
- Milliken, K. 2014. A compositional classification for grain assemblages in fine-grained sediments and sedimentary rocks. *Journal of Sedimentary Research*, **84**, <https://doi.org/10.2110/jsr.2014.92>
- Mnich, C.A. 2009. *Geochemical Signatures of Stratigraphic Sequences and Sea-Level Change in the Woodford Shale, Permian Basin*. Thesis.
- Montgomery, S.L., Jarvie, D.M., Bowker, K.A. and Pollastro, R.M. 2005. Mississippian Barnett Shale, Fort Worth basin, north-central Texas: gas-shale play with multi-trillion cubic foot potential. *American Association of Petroleum Geologists Bulletin*, **89**, <https://doi.org/10.1306/09170404042>
- Moore, D.M. and Reynolds, R.C., Jr. 1997. *X-Ray Diffraction and the Identification and Analysis of Clay Minerals*. 2nd edn, Oxford University Press, Oxford.
- Morris, A., Ferrill, D.A. and Henderson, D.B. 1996. Slip-tendency analysis and fault reactivation. *Geology*, **24**, 275–278, [https://doi.org/10.1130/0091-7613\(1996\)024<0275:STAAFR>2.3.CO;2](https://doi.org/10.1130/0091-7613(1996)024<0275:STAAFR>2.3.CO;2)
- Neuzil, C.E. 1994. How permeable are clays and shales? *Water Resources Research*, **30**, 145–150, <https://doi.org/10.1029/93WR02930>
- Neuzil, C.E. 2019. Permeability of clays and shales. *Annual Review of Earth and Planetary Sciences*, **47**, <https://doi.org/10.1146/annurev-earth-053018-060437>
- Neuzil, C.E. and Pollock, D.W. 1983. Erosional unloading and fluid pressures in hydraulically 'tight' rocks. *Journal of Geology*, **91**, 179–193, <https://doi.org/10.1086/628755>
- Nordgård Bolås, H.M. and Hermanrud, C. 2003. Hydrocarbon leakage processes and trap retention capacities offshore Norway. *Petroleum Geoscience*, **9**, <https://doi.org/10.1144/1354-079302-549>
- Nottvedt, A., Berglund, L.T., Rasmussen, E. and Steel, R.J. 1988. Some aspects of Tertiary tectonics and sedimentation along the western Barents Shelf. *Geological Society, London, Special Publications*, **39**, 421–425, <https://doi.org/10.1144/GSL.SP.1988.039.01.37>
- NEA 2022. *Clay Club Catalogue of Characteristics of Argillaceous Rocks - 2022 Update*, OECD Publishing, Paris.
- Nunn, J. 2012. Burial and thermal history of the haynesville shale: implications for gas generation, overpressure, and natural hydrofracture. *GCAGS Journal*, **1**, 81–96.
- Nygård, R., Gutierrez, M., Bratli, R.K. and Høeg, K. 2006. Brittle-ductile transition, shear failure and leakage in shales and mudrocks. *Marine and Petroleum Geology*, **23**, <https://doi.org/10.1016/j.marpetgeo.2005.10.001>
- O'Brien, G.W. and Woods, E.P. 1995. Hydrocarbon-related diagenetic zones (HRDZs) in the Vulcan sub-basin, Timor Sea: recognition and exploration implications. *The APPEA Journal*, **35**, 220–252, <https://doi.org/10.1071/aj94015>
- O'Brien, G.W., Quaipe, P., Cowley, R., Morse, M., Wilson, D., Fellows, M. and Lisk, M. 1998. Evaluating trap integrity in the Vulcan Subbasin, Timor Sea, Australia, using integrated remote-sensing geochemical technologies. In: Purcell, P.G. and Purcell, R.R. (eds) *The sedimentary basins of Western Australia. Proceedings of the West Australian Basins Symposium*, Perth, Australia, August 30–September 2, 237–254.
- Ohm, S.E., Karlsen, D.A. and Austin, T.J.F. 2008. Geochemically driven exploration models in uplifted areas: example from the Norwegian Barents Sea. *American Association of Petroleum Geologists Bulletin*, **92**, <https://doi.org/10.1306/06180808028>
- Osborne, M.J. and Swarbrick, R.E. 1997. Mechanisms for generating overpressure in sedimentary basins: a reevaluation. *AAPG Bulletin*, **81**, 1023–1041, <https://doi.org/10.1306/522B49C9-1727-11D7-8645000102C1865D>

- Ostanin, I., Anka, Z. and Di Primio, R. 2017. Role of faults in hydrocarbon leakage in the Hammerfest basin, SW Barents Sea: insights from seismic data and numerical modelling. *Geosciences (Switzerland)*, **7**, <https://doi.org/10.3390/geosciences7020028>
- Passsey, Q.R., Bohacs, K.M., Esch, W.L., Klimentidis, R. and Sinha, S. 2010. From oil-prone source rock to gas-producing shale reservoir - geologic and petrophysical characterization of unconventional shale-gas reservoirs. In: Society of Petroleum Engineers - International Oil and Gas Conference and Exhibition in China 2010, IOGCEC, Beijing, China, June 2010, <https://doi.org/10.2118/131350-ms>
- Pathak, M., Deo, M. and Levey, R. 2015. Examination of the generation of overpressure in the Eagle Ford. *Gulf Coast Association of Geological Societies Transactions*, **65**, 481–484.
- Paulsen, R.S., Birchall, T., Senger, K. and Grundvåg, S.A. 2022. Seal characterization and integrity in uplifted basins: Insights from the northern Barents Shelf. *Marine and Petroleum Geology*, **139**, <https://doi.org/10.1016/j.marpetgeo.2022.105588>
- Pawlewicz, M.J. 1989. *Thermal Maturation of the Eastern Anadarko Basin, Oklahoma*, <https://doi.org/10.3133/b1866C>
- Pedersen, T. and Bjørlykke, K. 1994. Fluid flow in sedimentary basins: model of pore water flow in a vertical fracture. *Basin Research*, **6**, 1–16, <https://doi.org/10.1111/j.1365-2117.1994.tb00071.x>
- Prada, A. and Civan, F. 1999. Modification of Darcy's law for the threshold pressure gradient. *Journal of Petroleum Science and Engineering*, **22**, 237–240, [https://doi.org/10.1016/S0920-4105\(98\)00083-7](https://doi.org/10.1016/S0920-4105(98)00083-7)
- Prasad, U., Franquet, J., Gonzalez, H.P., Moronkeji, D., Shouse, R., McGlynn, I. and Clawson, C.F. 2016. Integrated evaluation of Haynesville shale with special emphasis on anisotropy. In: 50th US Rock Mechanics Geomechanics Symposium 2016, Houston, Texas, June 2016.
- Quick, J.C. and Ressetar, R. 2012. Thermal maturity of the Mancos Shale within the Uinta Basin, Utah and Colorado. In: American Association of Petroleum Geologists Annual Meeting, Long Beach, California, USA.
- Raghavan, R. and Chin, L.Y. 2004. Productivity changes in reservoirs with stress-dependent permeability. *SPE Reservoir Evaluation and Engineering*, **7**, <https://doi.org/10.2118/88870-PA>
- Rickman, R., Mullen, M., Petre, E., Grieser, B. and Kundert, D. 2008. A practical use of shale petrophysics for stimulation design optimization: all shale plays are not clones of the Barnett Shale. In: Proceedings - SPE Annual Technical Conference and Exhibition, Denver, Colorado, USA, September 2008, <https://doi.org/10.2118/115258-ms>
- Ringrose, P.S., Mathieson, A.S. *et al.* 2013. The In Salah CO₂ storage project: lessons learned and knowledge transfer. *Energy Procedia*, **37**, 6226–6236, <https://doi.org/10.1016/j.egypro.2013.06.551>
- Ronov, A.B. 1983. *The Earth's Sedimentary Shell. AGI Reprint Series*, **5**.
- Salahshoor, S., Maity, D. and Ciezobka, J. 2020. Stage-Level Data Integration to Evaluate the Fracturing Behavior of Horizontal Wells at the Hydraulic Fracturing Test Site (HFTS): an Insight into the Production Performance, SPE/AAPG/SEG Unconventional Resources Technology Conference, Virtual, July 2020, <https://doi.org/10.15530/urtec-2020-3058>
- Schlömer, S. and Krooss, B.M. 1997. Experimental characterisation of the hydrocarbon sealing efficiency of cap rocks. *Marine and Petroleum Geology*, **14**, 565–580, [https://doi.org/10.1016/S0264-8172\(97\)00022-6](https://doi.org/10.1016/S0264-8172(97)00022-6)
- Schofield, J. 2016. *Relationships Between Observed Hydrocarbon Column Heights, Occurrence of Background Overpressure and Seal Capacity within North West Europe*. Doctoral dissertation, Durham University.
- Scott, D.W. 1992. *Multivariate Density Estimation: Theory, Practice, and Visualization*. John Wiley & Sons, New York.
- Scott, T.E. and Nielsen, K.C. 1991. The effects of porosity on the brittle-ductile transition in sandstones. *Journal of Geophysical Research*, **96**, 405–414, <https://doi.org/10.1029/90JB02069>
- Sellin, P. and Leupin, O.X. 2014. The use of clay as an engineered barrier in radioactive-waste management - a review. *Clays and Clay Minerals*, **61**, <https://doi.org/10.1346/CCMN.2013.0610601>
- Smalley, C., England, W.A., Muggeridge, A., Abacioglu, Y. and Cawley, S. 2004. Rates of reservoir fluid mixing: implications for interpretation of fluid data. *Geological Society Special Publication*, **237**, <https://doi.org/10.1144/GSL.SP.2004.237.01.07>
- Smye, K., Hamlin, H., Eastwood, R. and Mcdaid, G. 2019. Variability of geologic properties of shale gas and tight oil plays. *Gulf Coast Association of Geological Societies*, **8**, 191–209.
- Sone, H. and Zoback, M.D. 2013. Mechanical properties of shale-gas reservoir rocks - part 2: ductile creep, brittle strength, and their relation to the elastic modulus. *Geophysics*, **78**, <https://doi.org/10.1190/GEO2013-0051.1>
- Spencer, A.M. and Larsen, V.B. 1990. Fault traps in the Northern North Sea. *Geological Society, London, Special Publications*, **55**, 281–29, <https://doi.org/10.1144/GSL.SP.1990.055.01.13>
- Strapoć, D., Mastalerz, M., Schimmelmann, A., Drobnik, A. and Hasenmueller, N.R. 2010. Geochemical constraints on the origin and volume of gas in the New Albany Shale (Devonian-Mississippian), eastern Illinois Basin. *AAPG Bulletin*, **94**, <https://doi.org/10.1306/06301009197>
- Swarbrick, R.E. and Lahann, R.W. 2016. Estimating pore fluid pressure-stress coupling. *Marine and Petroleum Geology*, **78**, <https://doi.org/10.1016/j.marpetgeo.2016.10.010>
- Swarbrick, R.E. and Osborne, M.J. 1998. Mechanisms that generate abnormal pressures: an overview. *AAPG Memoir*, **70**, <https://doi.org/10.1306/M70615>
- Swarbrick, R.E., Lahann, R.W., O'Connor, S.A. and Mallon, A.J. 2010. Role of the Chalk in development of deep overpressure in the Central North Sea. In: Vining, B.A. and Pickering, C.S. (eds) *Petroleum Geology: From Mature Basins to New Frontiers: Proceedings of the 7th Petroleum Geology Conference*, Geological Society, London, <https://doi.org/10.1144/0070493>
- Tasianias, A., Martens, I., Bünz, S. and Mienert, J. 2016. Mechanisms initiating fluid migration at Snøhvit and Albatross fields, Barents Sea. *arktos*, **2**, <https://doi.org/10.1007/s41063-016-0026-z>
- Teige, G.M.G., Hermanrud, C., Wensaas, L. and Nordgård Bolås, H.M. 1999. The lack of relationship between overpressure and porosity in North Sea and Haltenbanken shales. *Marine and Petroleum Geology*, **16**, 321–324, [https://doi.org/10.1016/S0264-8172\(98\)00035-X](https://doi.org/10.1016/S0264-8172(98)00035-X)
- Thomas, L.K., Katz, D.L. and Tek, M.R. 1968. Threshold pressure phenomena in porous media. *Society of Petroleum Engineers Journal*, **8**, 174–184, <https://doi.org/10.2118/1816-pa>
- Tingay, M.R.P., Hillis, R.R., Morley, C.K., King, R.C., Swarbrick, R.E. and Damit, A.R. 2009. Present-day stress and neotectonics of Brunei: implications for petroleum exploration and production. *American Association of Petroleum Geologists Bulletin*, **93**, <https://doi.org/10.1306/08080808031>
- Vinard, P., Bobet, A. and Einstein, H.H. 2001. Generation and evolution of hydraulic underpressures at Wellenberg, Switzerland. *Journal of Geophysical Research: Solid Earth*, **106**, <https://doi.org/10.1029/2001jb000327>
- Wang, H.Y. 2017. What factors control shale-gas production and production-decline trend in fractured systems: a comprehensive analysis and investigation. *SPE Journal*, **22**, <https://doi.org/10.2118/179967-PA>
- Webster, R.L. 1984. Petroleum source rocks and stratigraphy of the Bakken Formation in North Dakota. In: Woodward, J., Meissner, F.F. and Clayton, J.L. (eds) *Hydrocarbon Source Rocks of the Greater Rocky Mountain Region: Rocky Mountain Association of Geologists*, 57–81.
- Wen, T., Castro, M.C., Ellis, B.R., Hall, C.M. and Lohmann, K.C. 2015. Assessing compositional variability and migration of natural gas in the Antrim Shale in the Michigan Basin using noble gas geochemistry. *Chemical Geology*, **417**, <https://doi.org/10.1016/j.chemgeo.2015.10.029>
- Wilson, T.K. and Bustin, R.M. 2017. *Unconventional Petroleum Systems Analysis of Upper Devonian Organic-Rich Shale Units in the Horn River and Liard Basins, Northeastern British Columbia and Adjacent Western Alberta: Preliminary Report*. Geoscience BC Summary of Activities 2016, Geoscience BC, Report 2017-1, 29–36.
- Winefield, P., Gilham, R. and Elsinger, R. 2005. Plumbing the depths of the Central Graben: towards an integrated pressure, fluid and charge model for the Central North Sea HPHT play. In: Dore, A.G. and Vining, B.A. (eds) *Petroleum Geology: North-West Europe and Global Perspectives - Proceedings of the 6th Petroleum Geology Conference*, The Geological Society, London, 1301–1315, <https://doi.org/10.1144/0061301>
- Wiprut, D. and Zoback, M.D. 2002. Fault reactivation, leakage potential, and hydrocarbon column heights in the northern north sea. *Norwegian Petroleum Society Special Publications*, **11**, [https://doi.org/10.1016/S0928-8937\(02\)80016-9](https://doi.org/10.1016/S0928-8937(02)80016-9)
- Wood, J.M. and Sanei, H. 2016. Secondary migration and leakage of methane from a major tight-gas system. *Nature Communications*, **7**, <https://doi.org/10.1038/ncomms13614>
- Yang, Y. and Aplin, A.C. 2007. Permeability and petrophysical properties of 30 natural mudstones. *Journal of Geophysical Research: Solid Earth*, **112**, <https://doi.org/10.1029/2005JB004243>
- Yang, S., Li, X., Zhang, K., Yu, Q. and Du, X. 2022. The coupling effects of pore structure and rock mineralogy on the pre-Darcy behaviors in tight sandstone and shale. *Journal of Petroleum Science and Engineering*, **218**, <https://doi.org/10.1016/j.petrol.2022.110945>
- Yardley, G.S. and Swarbrick, R.E. 2000. Lateral transfer: a source of additional overpressure? *Marine and Petroleum Geology*, **17**, [https://doi.org/10.1016/S0264-8172\(00\)00007-6](https://doi.org/10.1016/S0264-8172(00)00007-6)
- Zhang, C. and Rothfuchs, T. 2004. Experimental study of the hydro-mechanical behaviour of the Callovo- Oxfordian argillite. *Applied Clay Science*, **26**, <https://doi.org/10.1016/j.clay.2003.12.025>
- Zhang, C.L. and Talandier, J. 2023. Self-sealing of fractures in indurated clays: measured by water and gas flow. *Journal of Rock Mechanics and Geotechnical Engineering*, **15**, <https://doi.org/10.1016/j.jrmge.2022.01.014>
- Zhao, Y., Yang, H. *et al.* 2021. Choke management optimization for shale gas reservoirs with EDFM. In: 55th U.S. Rock Mechanics Geomechanics Symposium Virtual, 2021.
- Zhu, W. and Wong, T. 1997. The transition from brittle faulting to cataclastic flow: permeability evolution. *Journal of Geophysical Research: Solid Earth*, **102**, 3027–3041, <https://doi.org/10.1029/96jb03282>
- Zhu, G., Zhang, S., Liu, K., Yang, H., Zhang, B., Su, J. and Zhang, Y. 2013. A well-preserved 250 million-year-old oil accumulation in the Tarim Basin, western China: implications for hydrocarbon exploration in old and deep basins. *Marine and Petroleum Geology*, **43**, <https://doi.org/10.1016/j.marpetgeo.2012.12.001>